CHARACTERIZATION OF A MICROFLUIDIC BASED DIRECT-METHANOL FUEL CELL

By

ISAAC BENJAMIN SPRAGUE

A dissertation/thesis submitted in partial fulfillment of
the requirements for the degree of

MASTER OF SCIENCE IN MECHANICAL ENGINEERING

WASHINGTON STATE UNIVERSITY
School of Mechanical and Materials Engineering

August 2008

To the Faculty of Washington State University:

The members of the Committee appointed to examine the dissertation/thesis of ISAAC BENJAMIN SPRAGUE find it satisfactory and recommend that it be accepted.

_____
Chair

_____

_____

ACKNOWLEDGMENT

I am extremely grateful to my advisor Dr. Prashanta Dutta for a wonderful graduate school experience. His knowledge and understanding are what allowed me to fully enjoy my research. I also appreciate Dr. Su Ha for his help and teaching in electrochemistry and for his diligent assistance with my work. I'm grateful for his patients as I learned skills in a new discipline for me. I also am thankful to Dr. Konstantin Matveev for his time spent with me when I was a teaching assistant and for sitting on my committee.

Then there are my two colleagues in the micro scale thermal fluids laboratory. Without the friendship of Talukder Zaki Jubery and Dr. Jaesool Shim I could not have felt at home in graduate school. Their enthusiasm and intelligence helped raised my day to day efforts.

Also, I could not have even started without the help of Steve Brown and Joshah Jennings. Their assistance in the always tricky clean room was invaluable. Finally, I'd like to acknowledge all the other people whom are too numerous to name that helped me in my graduate studies.

I'd also like to thank the MME department for providing me with a teaching assistantship during my stay.

CHARACTERIZATION OF A MICROFLUIDIC BASED

DIRECT-METHANOL FUEL CELL

Abstract

by Isaac Benjamin Sprague, M.S.
Washington State University
August 2008

Chair: Prashanta Dutta

Increased demand for portable power has given new interest in research of small scale fuel cells. To meet this demand a new fuel cell type has emerged as an excellent system for micro scale application, the Laminar Flow Fuel Cell, LFFC. LFFC's are microfluidic based devices that can operate without a membrane, using laminar fluid mechanics to separate the fuel cell half reactions. In this thesis a direct methanol laminar flow fuel cell is fabricated and studied both experimentally and analytically.

The overall device performance is first briefly studied for stability and operating behavior. The characterization is done with performance curves and by monitoring open circuit potential. Some instability is found as well as performance trends based on methanol concentration, reactant flow rate, and electrolyte strength. The anode and cathode limitations are compared and it is found that the anode limitations are equivalent or greater.

The anode limitations have not been given as much attention as the cathode limitations. Therefore, the direct methanol anode is isolated in this work and studied in further detail. Anode polarization and electrochemical spectroscopy are used to better understand the observed behavior. The stability, methanol concentration effect, reactant flow rate effect, and electrolyte strength effect are the salient behaviors evaluated. The

results show that the methanol oxidation kinetics is greatly affected by these parameters. It is concluded that this relationship is due to a change in electric double layer structure. To better illustrate the role of the electric double layer an analytical model is used to simulate the behavior of the anode.

The important results are the demonstration of the poor stability of the laminar flow fuel cells, the adverse effect of methanol concentration and electrolyte flow rate on methanol oxidation kinetics, the dramatic benefit of a strong supporting electrolyte. This shows that the flowing electrolyte stream should be optimized just as any electrolyte would be in other fuel cell systems. It also shows the important consideration of the electric double layer and the roll it can play in fuel cell performance.

TABLE OF CONTENTS

Page

LIST OF FIGURES

Dedication

To my mother for without whom nothing would be possible

CHAPTER 1

Introduction

1.1 Motivation for LFFCs

As technology pushes forward more and more mobile electronics are becoming available. This gives rise to an increasing demand for better portable power solutions. These solutions must produce enough energy to power the mobile electronics with sufficient run time and yet be small enough to be portable. Current approaches are electrochemical devices such as batteries, electrochemical capacitors, and fuel cells. Batteries are well-established technology and have neared the peak of their optimization. However, the other options as a source for portable power are fairly juvenile and provide opportunity for vastly improved performance. It should be noted that fuel cell technology is also well established but not as a portable power source. In order for fuel cells to break into the portable power arena their size must be greatly reduced. This demand has given rise to recent work on miniaturized/portable fuel cell technology [1]. There have been efforts to miniaturize existing polymer electrolyte membrane (PEM) fuel cells. Given the small device sizes required this is not an easy or straightforward task. Fuel cells are assembled into stacks to obtain the necessary power, compounding the size constriction making the allowable size for each individual cell quite small. This provides quite a challenge for adapting current fuel cell technology.

However, a promising direction is the development of fuel cells that capitalize on the small scales for their fundamental operation. These microfluidic fuel cells use laminar flow to separate the fuel and oxidant streams. This eliminates the need for a membrane because the anode and cathode reactions are separated by laminar flow but protons are

still allowed to transport across the fluid-fluid interface. Although these laminar flow fuel cells (LFFC) cannot operate in larger scale applications they are better suited for miniaturization because they require no membrane which leads to a simplified cell design compared to the conventional polymer electrolyte membrane (PEM) fuel cell [1]. The device cost is also reduced without the expensive proton exchange membrane.

1.2 LFFC Fundamentals: An initial look

In order to provide a more rigorous definition of LFFC's it is necessary to establish the basic fundamentals of any fuel cell technology. A fuel cell is an electrochemical device that takes a thermodynamically favorable reaction and harnesses the chemical energy liberated in the form of electrical power. However, if the reactants are simply mixed and the reaction is allowed to proceed, no electrical work can be extracted. This is because the electrons are exchanged on the molecular level in an unorganized fashion through out the reaction and this is not useable work. Instead, a fuel cell takes this reaction and separates it into its two half reactions, generally fuel oxidation and oxidant reduction. These half reactions still need to be able to communicate to each other through the exchange of electrons and some positive ion, usually protons. This exchange of charge creates a complete circuit and the flow of electrons can be harnessed as electrical power.

The key to any fuel cell design is the separation of the half reactions that still allows the exchange of protons. Typical fuel cells use a physical barrier to separate the half reactions that is permeable by protons, a polymer electrolyte membrane for example. As mentioned previously LFFC's don't use a physical barrier such as a membrane, instead they capitalize on the behavior of fluids in a microchannel. In a microchannel the viscous

effects dominate the inertial effects. This is characterized by the extremely low Reynolds number, often much less than 1. This means that two aqueous streams fed side by side into a channel will only mix by diffusion and largely remain separated because of the laminar nature of the flow. Figure 1 shows a schematic of this behavior. In a LFFC one stream is an aqueous fuel solution and the second is an aqueous oxidant solution. Thus the reactions are separated while protons can still be exchanged due the ability of protons to conduct in solution.

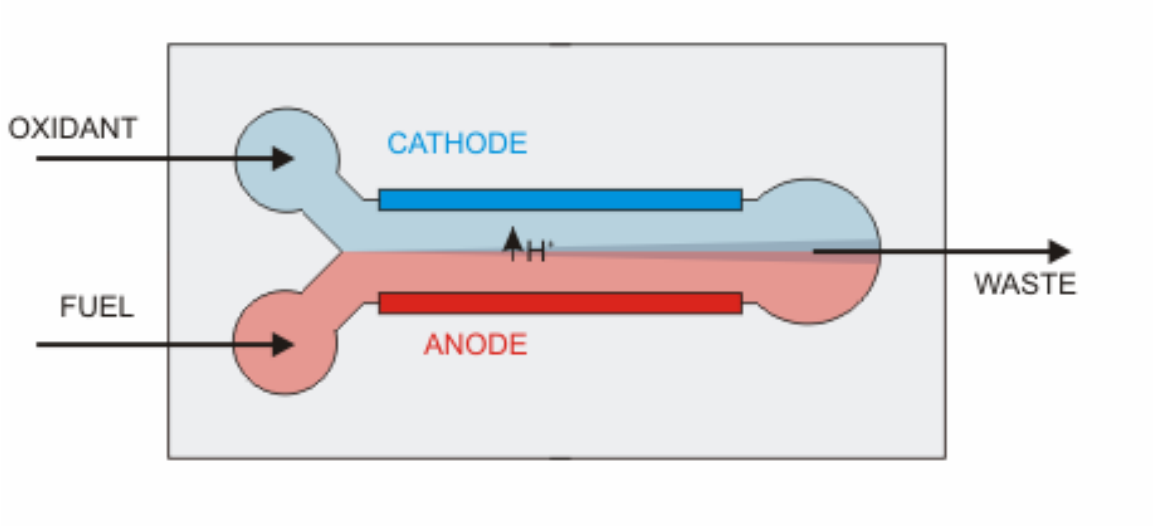

Figure 1.1 Schematic of Laminar Separation for LFFC

1.3 LFFC Experimental Developments

The concept was first demonstrated by Ferrigno *et al* [2] with a vanadium redox cell. Choban *et al* [3] did the initial characterization study on the operating behavior of LFFCs using a direct formic acid cell. They suggested performance limiting factors such as reaction kinetics, fuel crossover, and reactant transport to the electrodes. Choban *et al* [4] was able to confirm these limitations by using an external reference electrode to measure the potentials at the cathode and anode individually. They concluded that poor

oxygen replenishment at the cathode was the dominant limitation in LFFC performance. Also, the reactant replenishment limitation at the anode is negligible compared to the limitation at the cathode.

Some work has been done to reconfigure the geometry of LFFC's to improve overall device performance. Cohen *et al* [5] proposed a novel design for a LFFC using laminar flow between parallel plates instead of flow side by side in a channel. This planar channel design significantly increased the electrode surface area and allowed for easier fabrication of fuel cell stacks and arrays. Kjeang *et al* [6] proposed a unique architecture based on graphite rods as the electrodes to increase the active surface area. In a later work Kjeang *et al* [7] implemented a design where the reactant feeds were through porous electrodes. This device obtained excellent over all performance.

In membraneless LFFC, the fuel/oxidizing agent selection is flexible. Hasegawa *et al* [8] used this flexibility to explore new fuel possibilities. They used H_2O_2 in acidic and alkaline solutions as the fuel at the anode and oxidizing agent at the cathode. Kjeang *et al* [9] studied the use of vanadium as both the oxidizing agent and fuel source. This device showed good performance and relatively high fuel utilization. Cohen *et al* [10] also showed that LFFCs can be operated with a different pH for the anode and cathode electrolytes to achieve significantly increased open circuit potential (OCP). Choban *et al* [11] studied the effect of operating LFFCs in all acidic, all alkaline, and acidic/alkaline conditions. Despite showing better performance they concluded that acidic/alkaline mixed operation is not a promising avenue due to a significantly lower theoretical maximum energy density than all acidic or all alkaline conditions.

A lack of reactant replenishment at the cathode has been shown to be a large

performance limitation. This is in part because oxygen has a low concentration (2-4 mM) and diffusivity (2 x 10^{-5} cm^2/s) in an aqueous solution, Jayashree *et al* [12]. They presented an air-breathing LFFC that uses a gas diffusion electrode at the cathode. This significantly reduced the oxygen transport limitation because of higher concentration (10 mM) and diffusivity (2 x 10^{-1} cm^2/s) of oxygen in air. This provided substantial improvements in the device performance. Without the oxygen transport limitation, Jayashree *et al* [13] was also able to show increased performance by operating in alkaline conditions due to improved anode kinetics. Kjeang *et al* [14] studied the cathode limitation problem by using H_2O_2 as the oxidizing agent and showed significantly improved performance.

Some recent work has looked at other aspects of LFFCs. Lim *et al* [15] studied the electrode diffusion layer, specifically the electrode's geometry effect on performance. Sun *et al* [16] used a three stream channel with a third electrolyte stream separating the anode and cathode streams to eliminate fuel crossover. Li *et al* [17] demonstrated a simplified fabrication scheme and a fuel recycling system improving LFFC's commercial possibilities.

1.4 LFFC Fundamentals: A closer look

The scope of this work focuses less on device optimization and more on the fundamental science governing the behavior of LFFC's. It is therefore appropriate to take a closer look at the operating fundamentals of fuel cells. A fuel cell, as previously mentioned, is an electrochemical device. This means that the potential in the cell and the reaction kinetics are directly linked. In fact, the reaction is driven by a potential drop within the cell. The key to this relationship is the electrode-solution interface. The solid

electrode has a different potential than the bulk electrolyte solution and it is at the interface that there is a transition region for the potential distribution. This transition takes the form of the electric double layer whose structure directly controls the reaction kinetics. The double layer is generally theorized to consist of two parts, an inner compact double layer and the outer diffuse double layer. The inner layer, also sometimes referred to as the stern layer, is immediately adjacent to the electrode surface. In this layer are water dipoles and adsorbed anions. The potential drop across this layer is theorized to be linear and is the driving potential for the kinetics. The compact layer extends outwards into the solution to the plane of closet approach, or Outer Helmholtz Plane. This is the closest ions will get to the electrode surface without adsorbing and it is the reactant concentrations at this plane that affect the electrode kinetics. Beyond this lies the diffuse double layer. The electric double layer is a deviation from electroneutrality that arises because the charge in the electrode cannot equilibrate with the charge in the solution. Therefore, in the diffuse double layer the electrolyte ion concentrations will be imbalanced as the double layer compensates for this deviation. It is this microscopic interfacial phenomenon and how it changes that is essential the understanding of fuel cells, certainly including LFFC's.

1.5 Fundamental Studies of LFFC's

Performance characterization can only study the principal science behind the fuel cell operation only so far. To study the electric double layer and more specifically what role it plays in the performance limitations of LFFC's more powerful analytical tools are required. Experimental techniques, such as electrochemical impedance spectroscopy, can provide in situ characterization of the limitations. Impedance spectroscopy is a relatively

new and powerful method of characterizing many of the electrical properties of materials and their interfaces. Recently, this method has been used to evaluate the electrochemical behavior of anode and cathode electrodes, and electrolyte materials of hydrogen fuel cells and direct methanol fuel cells (DMFCs) [18-23].

Another approach to look into the fundamental principals of LFFC's is to model the system mathematically. Lots of work has been done on modeling PEM fuel cells [24-29]. Some of this work focuses on DMFCs [30-31]. Models for a DMFC anode have also been presented from a transport view [32] and a methanol oxidation kinetics view [33-35]. Some initial works has taken these principals and applied them to LFFC's. Bazylak *et al* [36] studied the behavior of a T-channel design numerically, focusing on the fuel utilization, which was shown to be poor. They proposed a tapered electrode design that would greatly increase fuel utilization and device performance. More analytic work was performed by Chang *et al* [37] who studied LFFC behavior of a Y-channel under different operating conditions. They showed that flow rate, channel geometry, and reactant concentrations all affect the cell performance and confirmed oxygen transport to the cathode as the dominant limitation. Chen *et al* [38] performed an analytic study of the planar channel design and showed that the device behavior and performance were comparable to the Y-channel designs. They concluded that a better method of increasing LFFC performance is needed than merely increasing the electrode surface area.

Typically the electric double layer is neglected in any fuel cell model. Instead, the entire potential difference between the solid electrode and the bulk electrolyte solution is taken to be the driving potential drop for the electrode kinetics. This is often referred to as the overpotential. However, there has been work done on solving Poisson's equation to

model the double layer in electrical chemical systems [39-40]. Several works have also considered the double layer's impact on electrode kinetics [41-43].

1.6 Research Goals

The approach in this work was to take a more fundamental look at the science behind LFFC's. This would lead to a better understanding of the performance limitations and therefore an improved ability to optimize devices for application.

Perhaps the most interesting concept to look at is the key difference in LFFC's from other fuel cell types. In a typical PEM fuel cell, the electrolyte is stationary where as in a LFFC the electrolyte is a flowing stream. This could potentially give rise to new unstudied performance limitations of LFFCs, as a moving electrolyte is unique. Also, the electrolyte and fuel streams in LFFC are the same; unlike conventional PEM fuel cell systems, where the fuel feed is physically separated from the electrolyte. This means that the electrolyte strength of the fuel stream plays an important role in the device performance for LFFC's. Therefore, the fuel selection has to be carefully considered as not all fuels are good electrolytes. For example, both the formic acid and methanol are simple hydrocarbon fuels, but methanol is not a good electrolyte. Often a strong electrolyte, such as sulfuric acid (H_2SO_4), can be added to the methanol solution to improve its poor electrolyte property. However, this might not always be acceptable in cases where an electrolyte is not available; such as fuel cells that operate off tree sap or when an electrolyte is not allowable in the cell such as biofuel catalysts that can be deactivated by the strong electrolytes. Also, it is scientifically important to understand how the electrolyte strength of the fuel stream affects the device performance, especially in the context of this unique case where it is also flowing. In this study, we focus on the

anode performance of LFFC's and investigate how it is affected by different flow rates of the anode stream. We selected methanol as our model fuel, because it allows us to study the performance of LFFC's in a case where the fuel has poor electrolyte properties. Also, sulfuric acid can be added to increase its electrolyte strength and understand how the presence of strong supporting electrolyte in the anode stream can alter its performance.

Other parameters that were considered were potential size effects or stability effects. In order for LFFCs to meet the power demands of portable power applications multiple cells will need to be stacked together. This means smaller cell channel sizes are needed to minimize the total volume of the stack. However, as they become microchannels, with the smallest dimension on the order of 1-10 μm, the operating behavior may change. It is well known in the MEMS community that scaling effects can affect device behavior in unexpected ways as surface effects and forces such as surface tension and viscous forces become dominant [44]. The long-term performances of microfluidic based direct methanol fuel cell are presented for the suitability of this device. If LFFCs are to become practical in portable power situations they must be stable over a long device life.

With this general motivation in mind the research goals are as follows:

1) To fabricate a LFFC and qualify it as an operational device
2) To briefly characterize the stability of the LFFC
3) To study the effect of the flowing electrolyte unique to LFFC's
4) To study methanol oxidation in a laminar flow device
5) To use an analytical model to describe the role of the interfacial phenomenon

CHAPTER 2

Experimental Procedures

2.1 Materials and Reagents

Pure methanol and sulfuric acid were purchased from Aldrich (St. Louis, MO). Platinum black and Platinum-Ruthenium black (50:50 atomic %) were procured form Alfa Aesar (Ward Hill, MA). Nafion (5% Solution) was obtained from Solution Technology Inc (Mendenhall, PA). Fluorescent dye, Rhodium-b, was obtained from Acros (Morris Plains, NJ). The fuel and oxidant solutions were prepared in the laboratory. For the fuel, pure methanol was diluted with Millipore water to a desired concentration. For the oxidant, sulfuric acid was diluted with Millipore water to a concentration of 0.5 M.

2.2 Basic Operation

To operate the fuel cell to study it experimentally an anode solution and cathode solution were supplied to the inlets. The waste, reaction by-products such as CO_2, water, and unutilized fuel were then collected in the exit reservoir. These solutions were pumped through the device using a syringe pump (74900-10, Cole-Parmer Instrument Company, Vernon Hills, IL) at flow rates of 1, 2, or 3 μL/min. In all tests performed, the flow rates of the anode and cathode streams were identical and equal to the flow rate specified by the operating conditions. Also, the cell was allowed to run for an hour for the flow to reach a steady state.

2.3 Fluorescent Imaging

To study the laminar flow separation of the anode and cathode fuel streams fluorescent imaging was used. To accomplish this, fluorescent dye was fed to one side of the cell, stream 1, and water to the other, stream 2. The images were captured using a fluorescent imaging microscope (Lecia DMLB, Bartels and Stout Inc., Bellevue, WA). Due to the limited field of view of the microscope the entire device could not be captured in a single image, so a series of images was taken and stitched together afterwards. Because the flow was steady state this method would not produce any inaccuracies.

2.4 Performance Characterization

To characterize the performance of the LFFC at the device level the cell was operated in as a complete fuel cell. This meant the anode was fed a methanol solution at various concentrations and flow rates and the cathode was fed an oxygen saturated 0.5 M sulfuric acid solution. The oxygen was dissolved to saturation in the sulfuric acid by bubbling oxygen gas for 30 minutes. For the voltage-current (V-I) curves and power density plots a resistance decade box (380400, Extech Instruments, Waltham, MA) was used to apply various loads to the cell. A multimeter (410, Extech instruments, Waltham, MA) was used to measure the voltage across the channel and a second multimeter (187, Fluke Corporation, Everett, WA) measured the current flowing in the circuit at each load. Figure 2.1 shows a schematic for the experimental set up. Before taking a data point for the V-I plot the voltage and current was allowed 5 minutes to stabilize at each load condition. In addition, to measure the hysteresis, both forward and backward scans were done for each set of performance data.

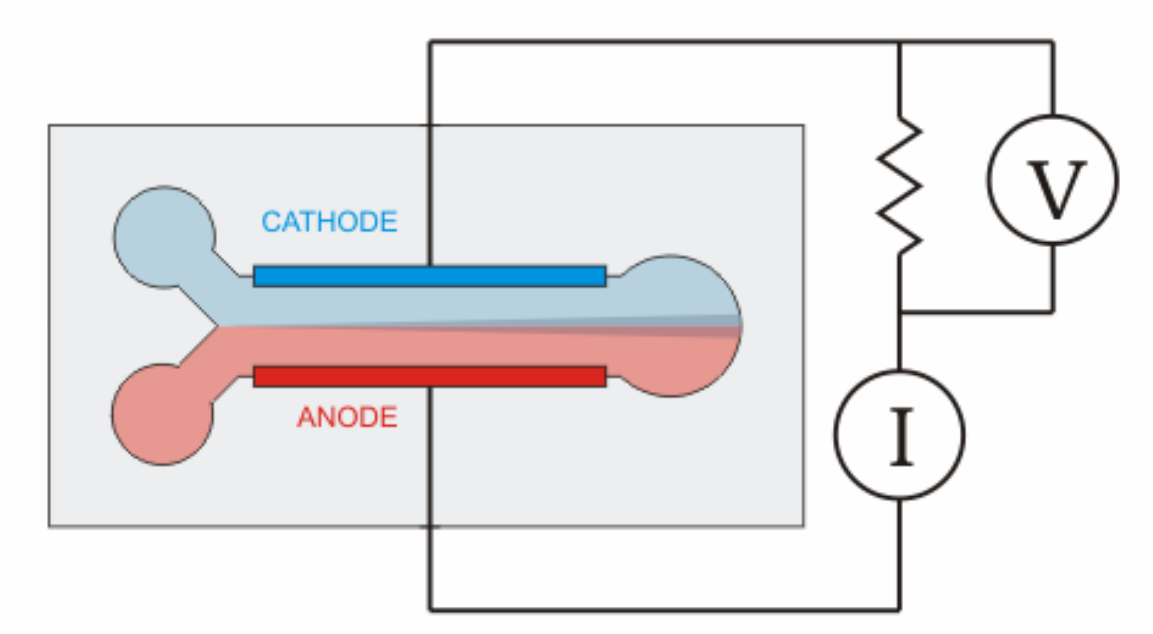

Figure 2.1 Schematic of the Experimental Set Up for Performance Characterization

2.5 Stability

An important aspect of the fuel cell behavior is the stability of its operation. It is critical to quantify this before any detailed experimental study can be performed. The stability of current at a fixed voltage is the standard measure of stability; however we did not have the sufficient equipment to study this. The stability we considered was how the OCP behaved with extended device operation time. To measure this stability the device was operated at an open circuit for a long duration of time and the OCP was recorded using a multimeter (410, Extech instruments, Waltham, MA) as a function of time. For these experiments the cell was fed with 1 M methanol solution to the anode and oxygen saturated sulfuric acid to the cathode and allowed to run constantly for 71 hours.

2.6 Anode Polarization

To study the effect of the anode flow rate with different electrolyte strengths on the anode performance of LFFC's, 1M methanol solution, with various concentration of sulfuric acid, was supplied to the anode inlet reservoirs. Methanol, in the absence of sulfuric acid, represented a fuel stream with poor electrolyte strength while a solution of methanol and sulfuric acid represented a stream with good electrolyte strength. 0.5 M sulfuric acid was fed to the cathode. Then, to characterize the anode performance, an anode polarization was performed. First, the fuel and oxidant solutions were supplied and the cell was allowed to reach steady state. Then, an incremental voltage was applied across the cell using a system power supply (6033A, Hewlett Packard, Palo Alto, CA). The applied voltage was increased from 0 to 800 mV in 50mV steps at 30 second intervals. The current in the circuit was measured with a multimeter (187, Fluke Corporation, Everett, WA). The experimental set up was the same as in Figure 2.1 except that the voltage was applied instead of measured, meaning the load resistance had no relevance in this experiment. In this configuration the anode reaction is methanol oxidation. The cathode, however, acts as a dynamic hydrogen reference electrode (DHE), providing both a counter and reference electrode for the study. This means that the anode polarization test allows the measure of performance limitations associated with the anode electrode only. An anode polarization was also done for various concentrations of methanol in the fuel solution.

2.7 Electrochemical Impedance Spectroscopy

For the electrochemical impedance spectroscopy, the cell was again supplied with fuel and oxidant and allowed to reach a steady state flow. 0.5M of sulfuric acid was

supplied to the cathode. This eliminated the effect of the cathode impedances, and to investigate only the anode impedances of the cell as the cell operation parameters are varied.

To perform the measurements the cell was hooked up to an electrochemical interface (SI 1287, Solartron Analytical, Farnborough Hampshire, UK) which was connected to an impedance/gain-phase analyzer, (SI 1260, Solartron Analytical, Farnborough Hampshire, UK) as shown in Figure 2.2.

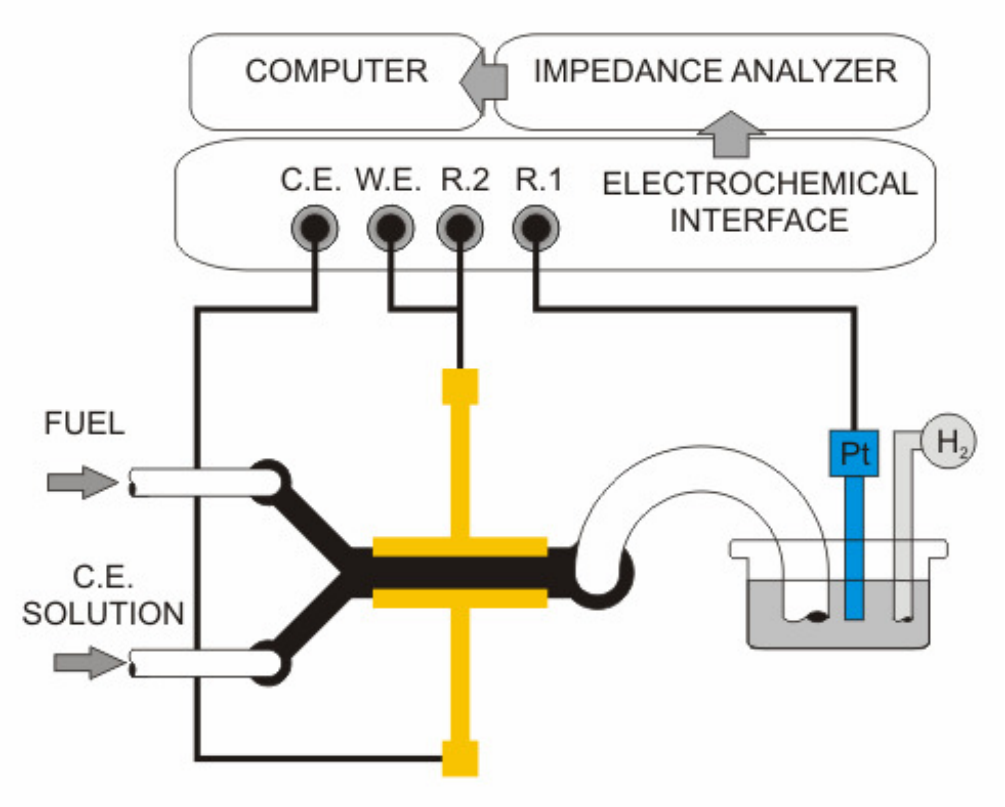

Figure 2.2 Schematic of Experimental Set Up for Electrochemical Impedance Spectroscopy

The impedance analyzer was linked to a computer and controlled using ZPlot (Scribner Associates Inc, Southern Pines, NC). The cell was connected to the electrochemical interface as a three terminal cell. To accurately control the potential

across the electrode being studied, a reference electrode was needed in the electrolyte. Due to the sensitivity of this technique it was beneficial to separate the reference electrode from the counter electrode in these experiments. This was accomplished with a standard hydrogen reference electrode in the waste beaker. The beaker was filled with 1M sulfuric acid and hydrogen was bubbled onto a platinum wire. This set up is appropriate as there is a direct electrolyte connection between the reference electrode and working electrode. Also, because no current flows between the working electrode and the reference electrode, any potential drop between the two electrodes is negligible. Next the working electrode and second reference electrode leads of the interface were both connected to the anode side of the device. Finally, the counter electrode lead was connected to the cathodic side of the cell. To avoid inductance among lines, short lines were used and the no wire was tangled.

To obtain the results of impedance measurement, a frequency sweep was performed with potential as the input, and current as the measured quantity. The amplitude of the AC potential signal was 50 mV and the frequency was swept between 1 MHz and 1 Hz. The device was too unstable to get data below 1 Hz with sufficient repeatability. As no trends in impedance based on load were noticed, all scans were performed at open circuit potential. All scans were performed four times and the average data is presented.

2.8 Equivalent Circuit Model

Electrochemical impedance spectroscopy is a powerful tool that can provide a lot of revealing information, however the data is difficult to analyze directly. By using an equivalent circuit to recreate the measured impedance spectra, the information learned

from the experiments can truly be maximized. It is important to use the correct equivalent circuit to analyze the data. The equivalent circuit used to describe the anode electrode in this study is shown in Figure 2.3. It is well known that the equivalent circuit for fuel cell electrode kinetics is a resistor in parallel with a capacitor. The resistor represents the resistance to charge transfer across the solution electrode interface, $R_{anode,ct}$. The capacitor represents the capacitance between the electric double layer and electrode surface, C_{dl}. This kinetic circuit is then connected in series with R_{ele}, which represents the resistance to ion conduction in the electrolyte [45]. The final component is the geometric capacitance, or C_{geo}.

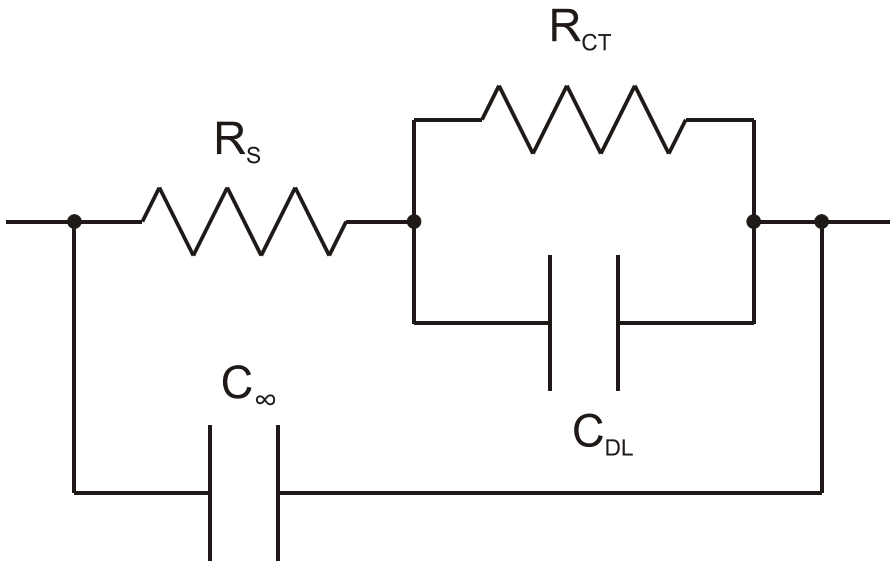

Figure 2.3 Equivalent Circuit Model Used for Electrochemical Impedance Spectroscopy Analysis

Often C_{geo} is neglected from fuel cell circuits because it doesn't affect the frequency ranges studied, but for our case it can't be neglected as our frequency range includes 1 MHz [45]. This capacitance represents the fact that a LFFC's geometry forms a capacitor because two electrodes separated by a gap is essentially a capacitor. C_{geo}

should therefore be constant throughout this study. The Warburg impedance that occurs from diffusion limitations was neglected from the equivalent circuit model, because of the unstable device behavior at low frequency that didn't allow for acceptable data fitting. Therefore, the circuit fitting was done in a frequency range that was not affected by diffusion limitations. In this study, the Warburg impedance was a significant factor only for methanol with high concentration of sulfuric acid. In general, the cell was not diffusion limited. The fitting was performed by ZView (Scribner Associates Inc, Southern Pines, NC) with an accuracy of less then 2% error on each calculated value.

CHAPTER 3

Device Design and Initial Characterization

3.1 Design of LFFC

A device schematic is shown in Figure 3.1. The device was designed primarily to study the anode performance and limitations of LFFC's. The straight channel is 3 mm wide, however because the anode is being isolated for this study, the large width is not as important an issue. A second series of devices were fabricated with a 1 mm wide straight channel to study the effect of channel width all other dimensions remained the same. The other dimensions of the straight channel are 10 μm tall and 25 mm long, while the branch channels of the Y-junction are 1.5 mm wide and 5 mm long. Each reservoir is 5 mm in diameter.

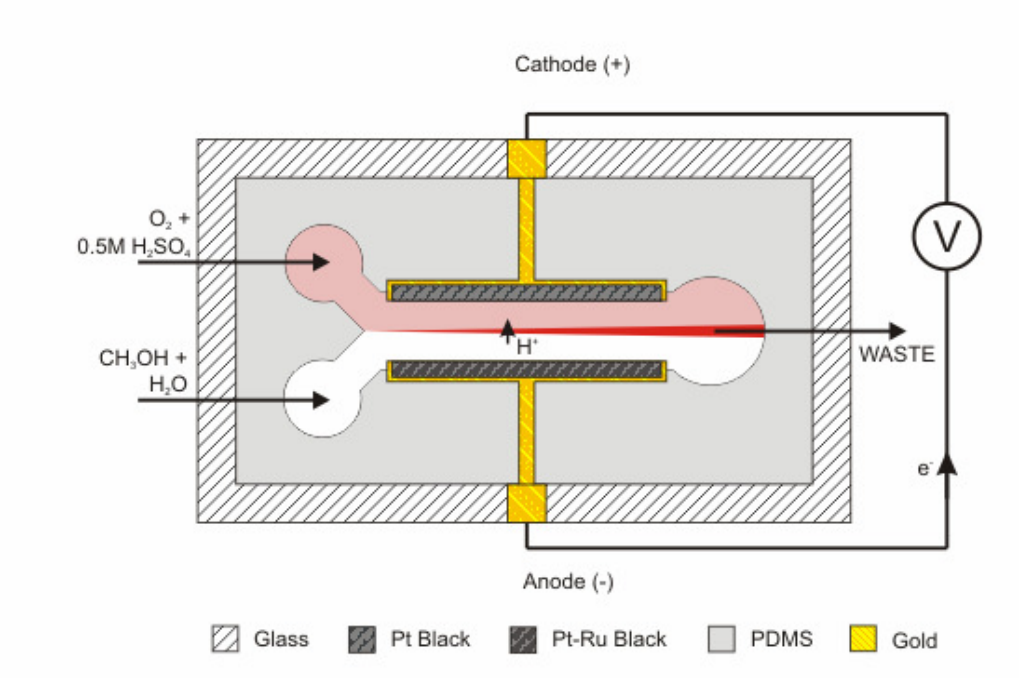

Figure 3.1 Schematic of the LFFC Device

The LFFC was made with polydimethylsiloxane (PDMS) on a glass substrate. The gold electrodes are deposited on both sides of the channel with dimensions of 20 mm long, 0.5 mm wide and 375 nm thick. The anode and cathode catalysts are Pt-Ru Black and Pt Black respectively. Pt-Ru was used at the anode to limit CO poisoning, which is a poisoning intermediate for methanol oxidation.

3.2 Fabrication of Laminar Flow Fuel Cell

Figure 3.2 shows the steps involved in fabricating the device. A positive mold was made on a glass slide, show in Figure 3.2.A, using standard photolithographic techniques. Briefly, photoresist was spun on, seen in Figure 3.2.B, and patterned using positive lithography, Figure 3.2.C&D. PDMS prepolymer and curing agent (Sylgard 184, Dow Corning Inc., Midland, MI) were mixed with a ratio of 10:1 and poured onto the mold. The PDMS then degasses for 2 hours at 0.001 Torr and baked at 80ºC for 3 hours, Figure 3.2.E. The PDMS channel was removed from the mold and trimmed to size. The reservoirs were formed using a 20 gauge needle to punch out a hole in the PDMS, illustrated in Figure 3.2.F. The gold for the electrode was sputtered to 375 nm thick layer using a 10 nm TiW layer as an adhesion layer, Figure 3.2.G. The electrodes were then formed by standard gold patterning techniques, Figure 3.2.H. Catalyst inks were prepared by mixing appropriate amounts of catalyst particles, Millipore water, and Nafion® solution. This mixture was sonicated and applied to the gold electrodes using a brush and heat lamp to evaporate the excess water, Figure 3.2.I. The PDMS channel was exposed to oxygen plasma and placed on a glass slide, seen in Figure 3.2.J, using slight pressure and allowed to sit for 24 hours creating a permanent bond and the final device, Figure 3.2.K. Capillary tubes were than glued in the reservoirs for transport of reactants and products to

and from the device, respectively. Wires were cold soldered using silver conductive epoxy (MG Chemicals, Burlington Ontario) to form the electrical leads of the fuel cell.

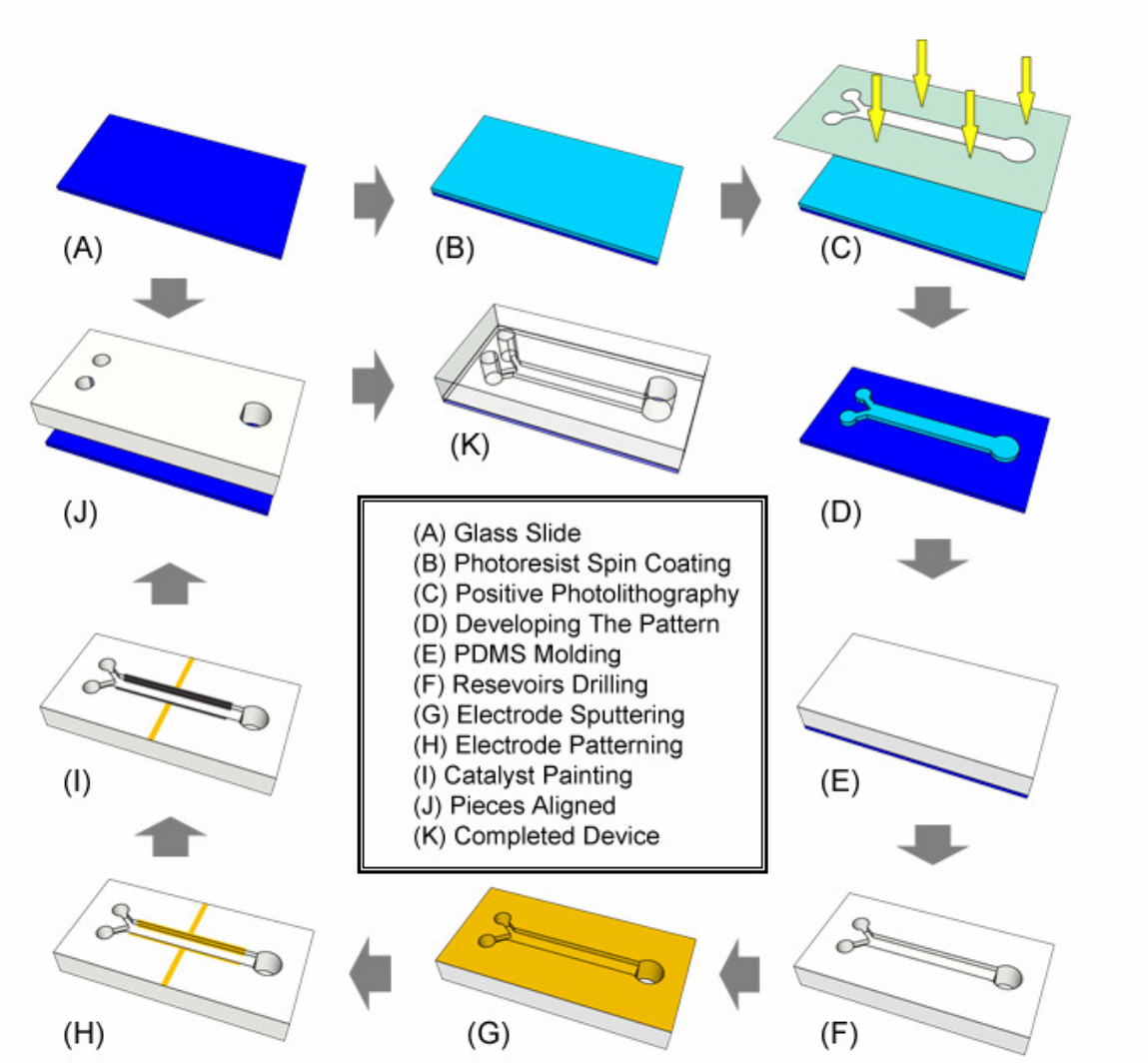

Figure 3.2 Fabrication Sequence of Laminar Flow Fuel Cell

3.3 Methanol and Oxygen Crossover

In general, fuel crossover can occur in LFFCs by diffusive mixing from one electrode to another, which creates mixed potentials and decreases the cell efficiency. To study the potential of this and the laminar separation in general fluorescent imaging was used along with a simple analytical model of the cross channel mixing. The theoretical

transverse diffusive broadening at a specific distance (x) along the channel is given by [37,46]:

$$\delta(y) \propto \left(\frac{DHx}{U} \right)^{1/3} \tag{3.1}$$

where D is the diffusivity of the species, H is the channel height, and U is the average fluid velocity in the channel. In this study, we used a very low aspect ratio planar microchannel (10 μm high and 3 mm wide). Hence, the theoretical transverse diffusive broadening will be much smaller than the channel width as shown in Figure 3.3.A. For instance, our channel with a diffusivity coefficient of (1 x 10^{-9} m^2/s) and an average velocity of 1.11 mm/s (corresponding with a reactant flow rate of 1 μL/min) the transverse diffusive broadening at the exit (x = 25 mm) is 60.8 μm. Thus, the fuel crossover can be prevented in our planar system.

We also observed the mixing behavior for our system. Figure 3.3.B-D show fluorescent images taken at flow rates between 1 and 3 μL/min. The catalyst layer and side walls can be seen in the images. Near the outlet of the channel the image is obscured by interference from the glue that was used for connecting outside capillary tubes. In the fluorescent images, there appears to be very little mixing at the interface and that the fluorescent dye has not traveled across the channel a significant amount for any of the flow rates used. Figures 3.3.B-D confirms that the mixing zone is very small relative to the channel width and crossover is not an issue in our devices.

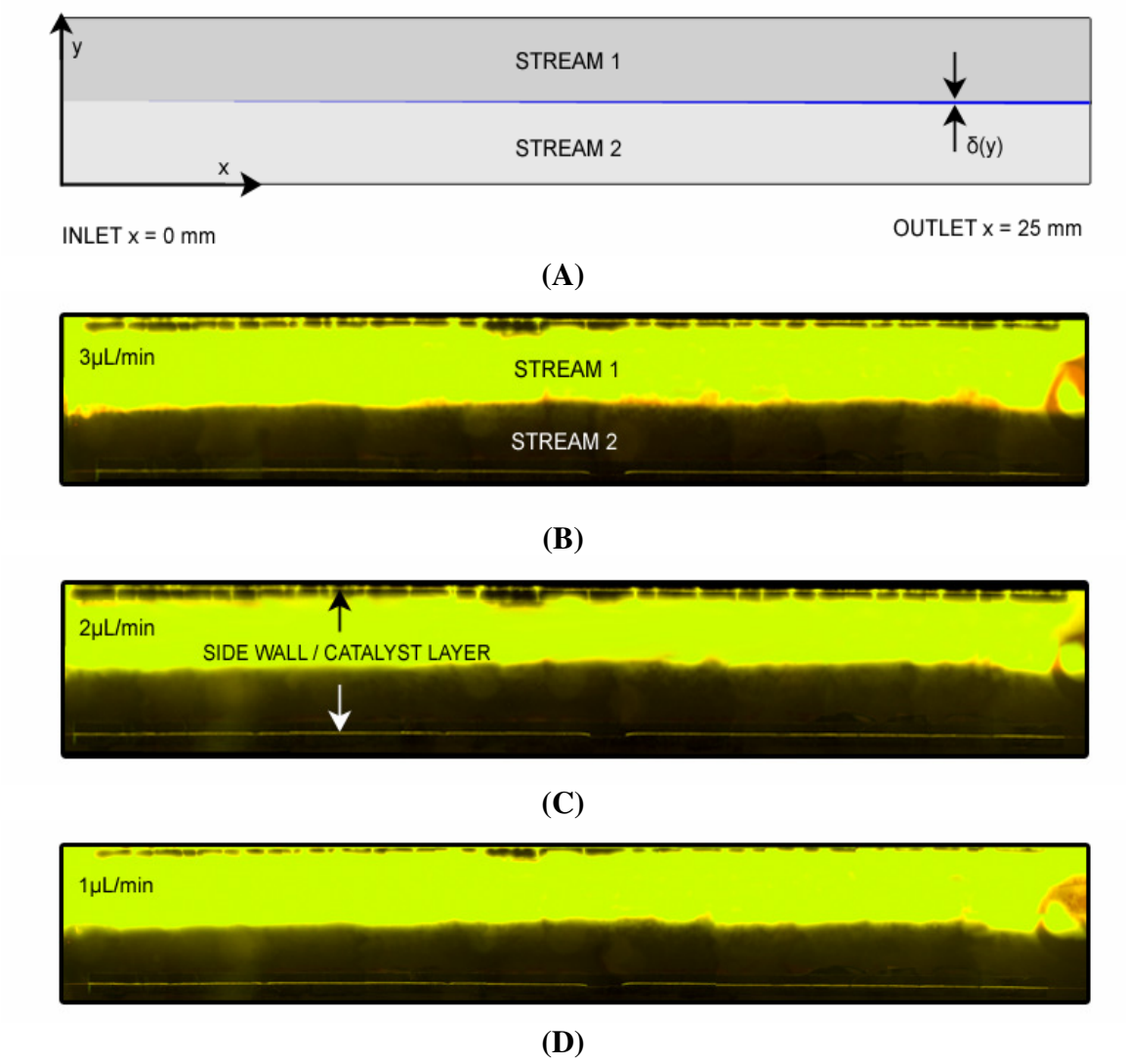

Figure 3.3 (A) Theoretical transverse diffusive broadening along the channel. Florescent images of the two streams in the main channel at (B) 1 μL/min, (C) 2μL/min and (D) 3μL/min. Rhodium-b was used as the dye in stream 1 to show the amount of mixing into stream 2.

3.4 Performance Characterization

A good place to start in any study of a fuel cell technology is to characterize the overall device performance. For the overall operation the anode was supplied methanol fuel solution and the cathode supplied oxygen saturated sulfuric acid as the oxidant.

Therefore the anode reaction is methanol oxidation:

$$CH_3OH + H_2O \longrightarrow 6H^+ + 6e^- + CO_2 \tag{3.2}$$

The cathode reaction is oxygen reduction:

$$1.5O_2 + 6H^+ + 6e^- \longrightarrow 3H_2O \tag{3.3}$$

Typically a fuel cell's performance is measured with a V-I plot and a power density plot such as the ones shown in Figure 3.4 for various methanol concentrations. The cell has decreased performance for increasing concentrations of methanol. This is an interesting result because it is unclear whether methanol oxidation has a positive or negative reaction order. Reports of both can be seen in the literature [33-35, 47]. In both cases the anode of a PEM fuel cell is studied but they suggest different methanol oxidation kinetics. However, the results presented in this work are some what unexpected anyways due to the severity of the negative correlation. The performance for the fuel cell operating with 0.5 M methanol is quite good. Where as the performance for the fuel cell operating with 4 M methanol is hardly anything and probably couldn't even be considered a useable device.

There are some other factors that may be considered to explain this relationship such as fuel cross over, reactant replenishment, and ohmic drop in the bulk solution. Higher methanol concentrations cause higher driving forces for diffusion. Therefore the amount of diffusion mixing increases. This impacts the reactant replenishment in a positive manner, the reactants are supplied to the electrode better, and fuel cross over in a negative manner, the fuel makes it further towards the cathode. However since it was shown that there is absolutely no risk of cross over in the presented device design neither of these phenomenon are likely to affect the performance significantly.

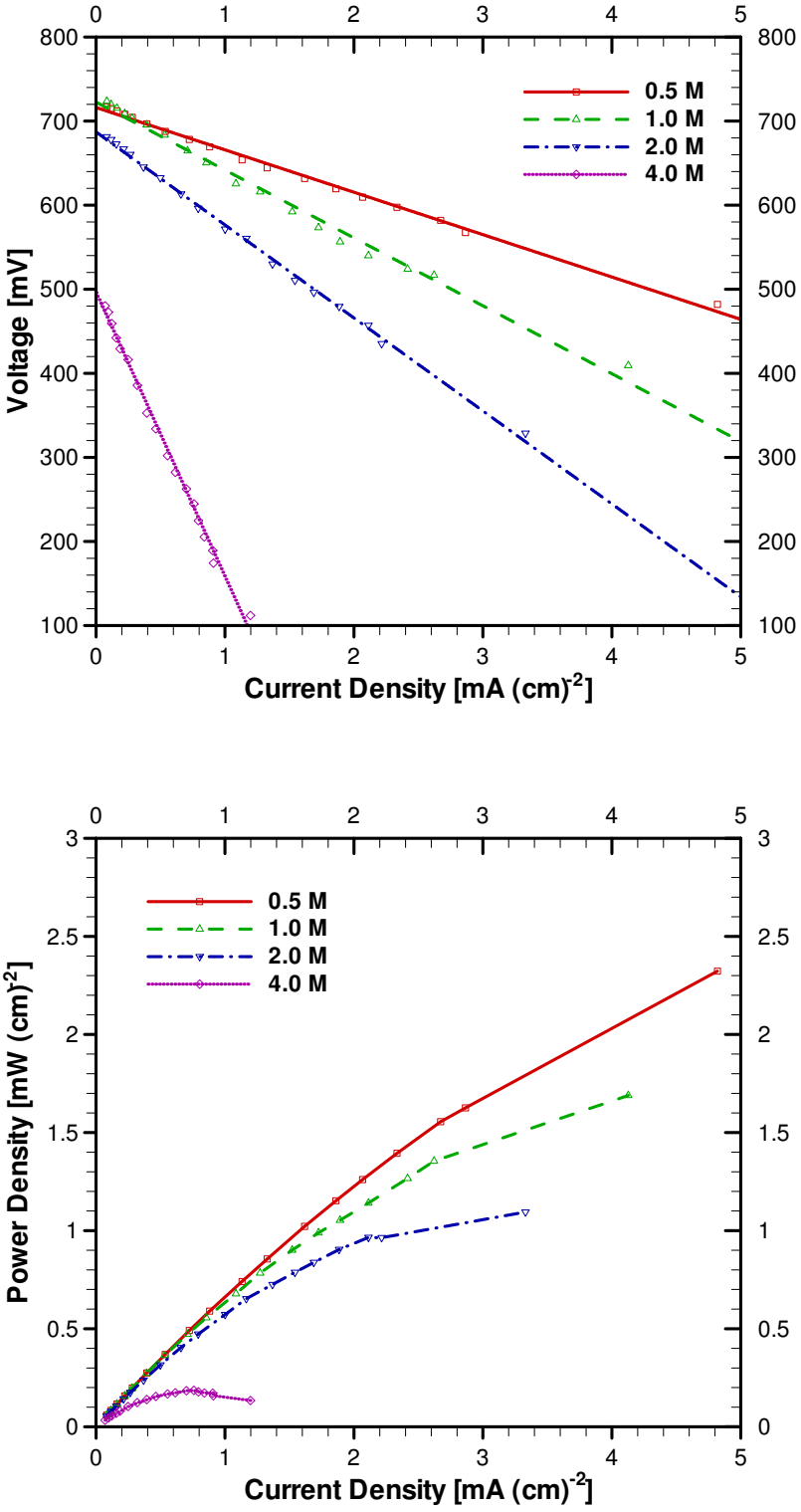

Figure 3.4 (A) V-I and (B) Power Density Performance of the Laminar Flow Fuel Cell Operating at 0.5, 1, 2, and 4 M Methanol Concentrations

Protons have a high mobility in aqueous solutions that decreases substantially as percent mass of methanol increases in the solution. This means that for the 4 M case the fuel stream has a much worse electrolyte conductivity. However, the scale of this potential drop needed to conduct protons is not large enough to be solely responsible for the decrease in performance.

Another approach to study the methanol concentration effect is to do an anode polarization. An anode polarization requires the device to be operated as a half cell, where the anode reaction remains methanol oxidation but the cathode becomes a dynamic hydrogen reference electrode. To do this the cathode is fed sulfuric acid with no oxygen and the reaction then becomes the hydrogen reduction reaction:

$$2H^+ + 2e^- \longrightarrow H_2 \tag{3.4}$$

Figure 3.5 shows a polarization plot for the various methanol concentrations. It supports the previous finding that increased methanol concentration has a severe negative impact on the anode performance. It is difficult to extract any more of an explanation out of this data. A closer look with a more powerful technique could provide further insight. However, it is noted that the methanol concentration effect can be eliminated by adding a strong supporting electrolyte to the fuel solution. Figure 3.6 shows anode polarization data for the various methanol concentrations with the addition for 0.5 M sulfuric acid to the fuel solution. With the addition of sulfuric acid the anode current density produced is much greater at higher applied potentials. Also, it can be seen that there is no longer any statistically significant trend associated with methanol concentration.

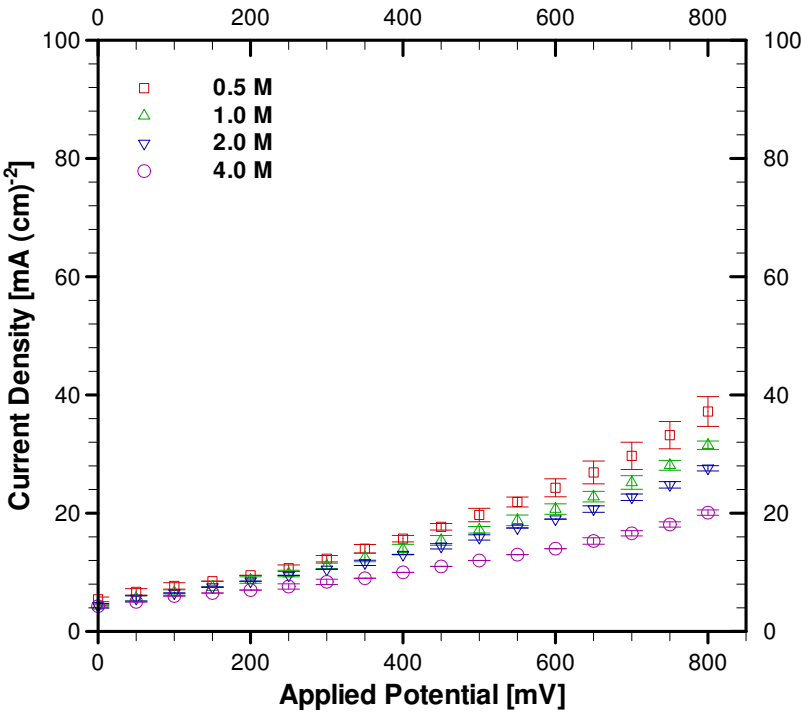

Figure 3.5 Anode Polarization of the Laminar Flow Fuel Cell Operating at 0.5, 1, 2, and 4 M Methanol Concentrations

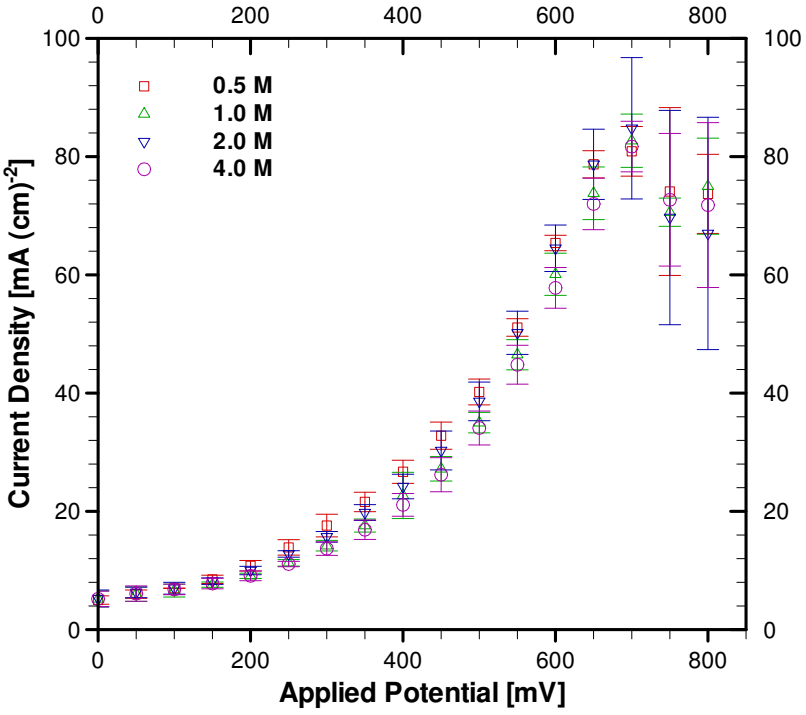

Figure 3.6 Anode Polarization of the Laminar Flow Fuel Cell Operating at 0.5, 1, 2, and 4 M Methanol Concentrations and 0.5 M Sulfuric Acid Added to the Fuel Stream

An interesting observation of Figure 3.6 is a high applied potential the cell becomes mass transport limited. Not enough methanol can be supplied to the anode to maintain the high kinetic current.

The device performance was also studied with different reactant flow rates. Figure 3.7 shows the performance curves for flow rates of 1, 2, and 3 μL/min. The overall device performance decreases with increasing flow rate. This is quite interesting because at first it would seem that the performance should improve with faster flow rates that provide better reactant replenishment to the electrode. This negative trend will be presented in greater detail in Chapter 4.

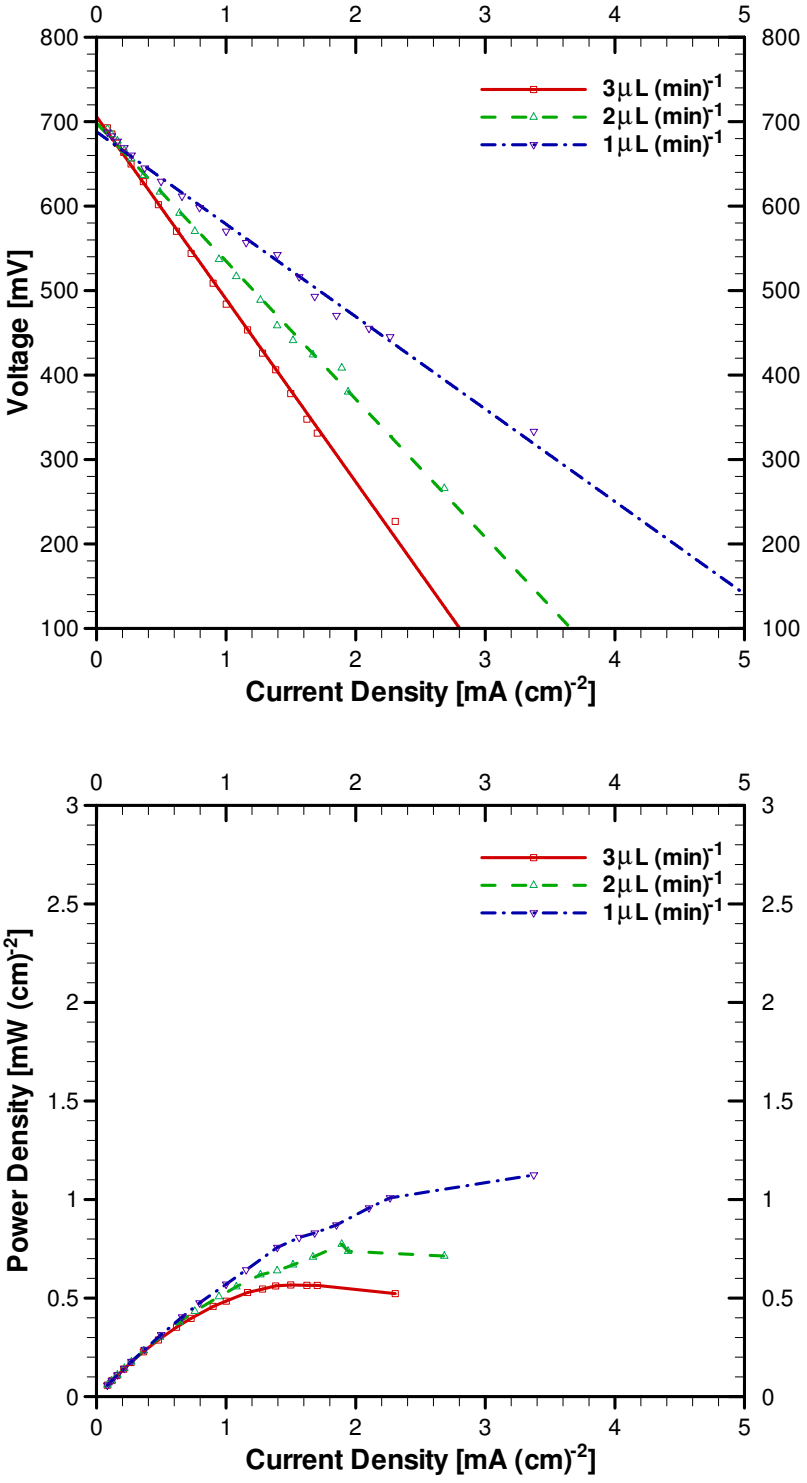

Figure 3.7 (A) V-I and (B) Power Density Performance of the Laminar Flow Fuel Cell Operating with Flow Rates of 1, 2, and 3 μL/min

3.5 Stability

An important device characteristic that has not been presented for LFFCs is the long-term stability. Figure 3.8 shows that the OCP behavior over time. It is interesting to note that for regular fuel cells the OCP tends to fluctuate but in our device the change in OCP was a smooth steady (no fluctuation) decrease with time. The cell took about an hour to develop the steady state flow and reach the peak OCP of 700 mV. Then the OCP began to decrease, initially the rate at which it drops is rather quick, but as time increases it dropped less rapidly. Although the rate of decent of the OCP slows down, the OCP never stabilizes at a steady state value. This drop is either caused by the device degradation or some phenomenon in the device operation.

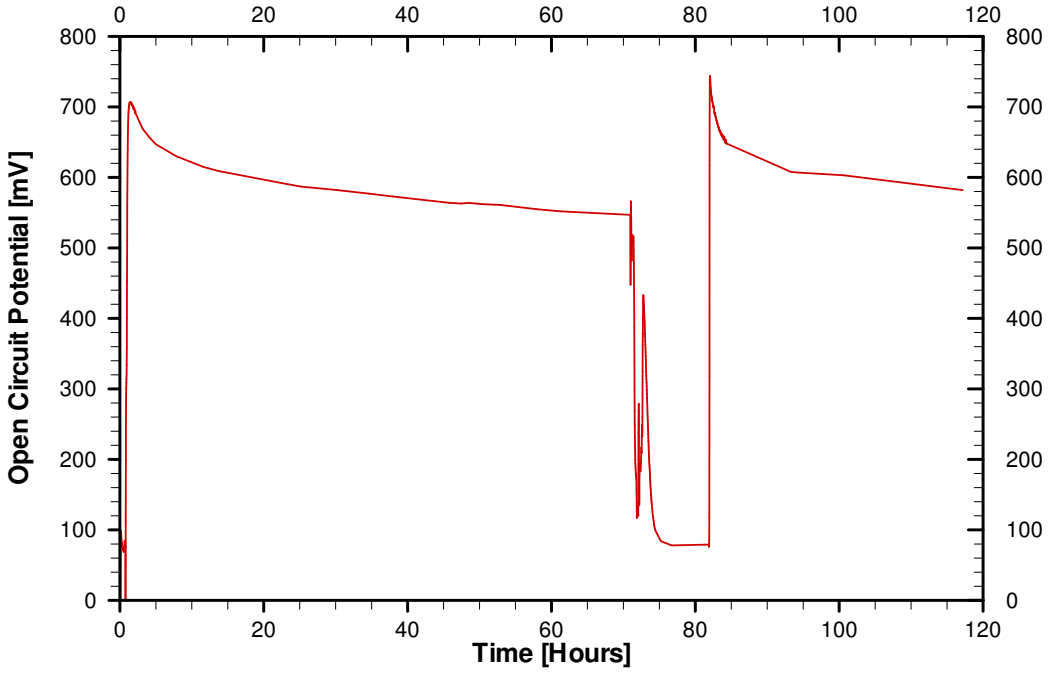

Figure 3.8 Long Term Stability Behavior of the Open Circuit Potential of a LFFC

At 71 hours the fuel and oxidant flow was stopped and both the anode and cathode were

fed with Millipore water. Water was fed to the device for 12 hours which flushed out the cell, allowing it to be restarted. By restarting a flushed out device it can be determined if the OCP drop is caused by device degradation or by an operational characteristic. At the 83 hour, 1 M methanol and oxygen saturated sulfuric acid were again fed to the anode and cathode respectively. The device was run for another 36 hours while OCP was again monitored. The magnitude and behavior of the OCP is equivalent to the original 36 hours. It can be concluded that the device had not degraded and that there is an operational phenomenon in LFFCs that causes the OCP to drop. One explanation that applies to this same trend in regular macro scale PEM fuel cells is catalyst poisoning due to CO by-product of methanol oxidation. However, we used the bimetallic catalyst Pt-Ru specifically to limit this. Also, at open circuit potentials, there is very little current draw generating very little CO intermediate, so catalyst poisoning is most likely not the cause. Further investigation would be required before definite phenomena could be cited as the cause for the instability in our LFFC.

CHAPTER 4

The Flowing Electrolyte

4.1 Methanol Flow Rate Effect in Absence of H_2SO_4 on Methanol Oxidation Kinetics

First the anode performance was studied with a flowing methanol stream in the absence of sulfuric acid, leading to a flowing poor electrolyte. It was found that at different flow rates the anode performance changed. Figure 4.1 shows the anode polarization plots of a LFFC using 1M methanol in the absence of sulfuric acid at the various flow rates.

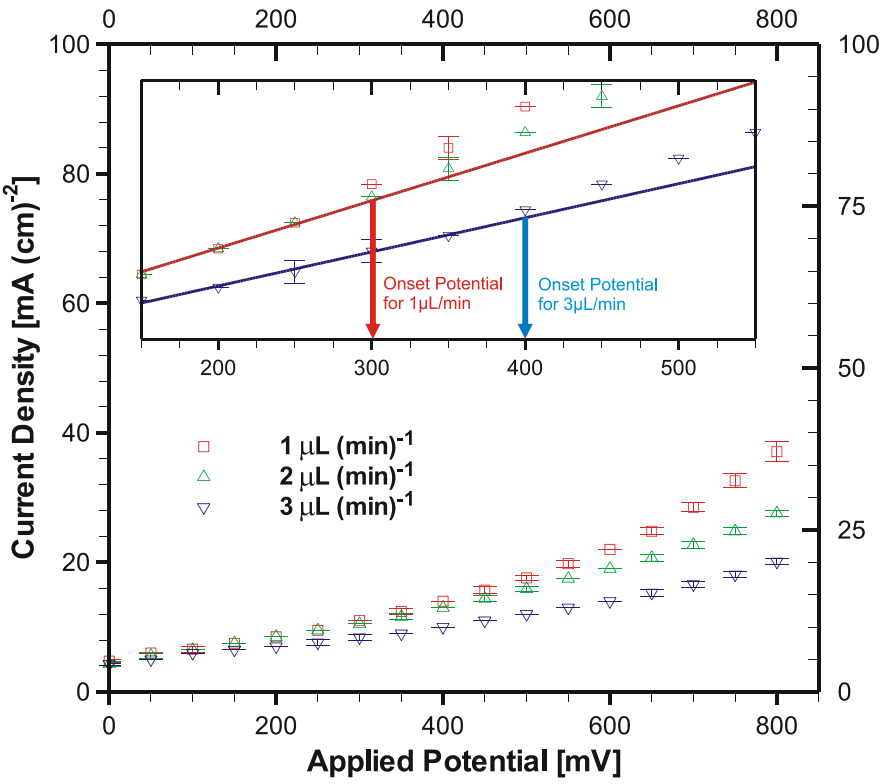

Figure 4.1 Anode Polarization of the Laminar Flow Fuel Cell Operating at 1, 2 and 3 µL/min Flow Rates. 1M methanol solution with no sulfuric acid was fed to the anode. The PtBl based cathode was set-up as a dynamic hydrogen reference electrode/counter electrode

It shows that as the methanol flow rate increases the anode performance decreases. This is not an expected result as higher flow rates would usually mean better fuel replenishment and therefore better performance [3]. These results would indicate that a higher methanol flow rate adversely affects methanol oxidation kinetics. In Figure 4.1, the methanol flow rate of 3 μL/min shows the onset potential of methanol oxidation at around 400 mV vs. RHE. The onset potential is defined as the applied anode potential that leads to the exponential increase in the anode current density. However, as the flow rate decreases from 3 to 1 μL/min, the onset potential of methanol oxidation decreases from 400 to 300 mV vs. RHE. This trend suggests that the increased flow rate of methanol negatively affects the methanol oxidation kinetics.

Although it is not convincing to make this conclusion from the anode polarization data alone, the electrochemical impedance spectroscopy data can provide further insight into the performance drop at higher methanol flow rates. Figure 4.2.A shows the anode impedance spectrum for different methanol flow rates in the absence of sulfuric acid. At first glance, it shows that as the methanol flow rate increases anode resistance also increases. Also, because the change in impedance is primarily in the second and larger hemi circle, it would seem that this increase in impedance is associated with methanol oxidation kinetics.

For a more rigorous analysis of the impedance spectra, the data was fit to the equivalent circuit model. Figure 4.2.B shows the fitted results for the R_{ele} and $R_{anode,ct}$. Figure 4.2.B clearly shows that $R_{anode,ct}$ increases with increasing flow rate. It also shows that R_{ele} is essentially unchanged with methanol flow rate, an expected result from theory.

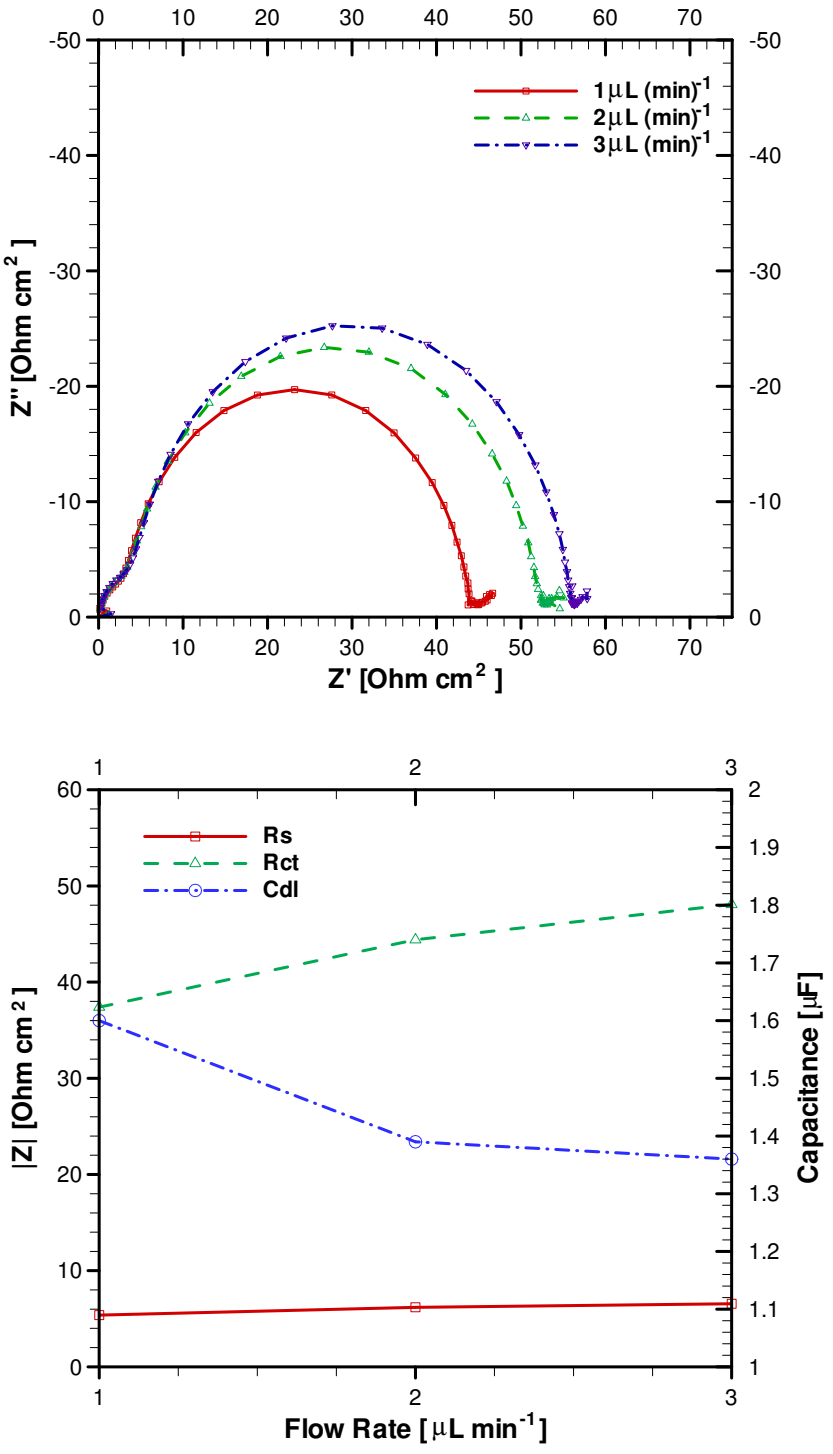

Figure 4.2 (A) Anode impedance spectra showing the methanol flow rate effect. Methanol concentration was fixed at 1M and no sulfuric acid was added. (B) The equivalent circuit fit values of solution resistance (R_{ele}), anode charge transfer resistance (R_{ct}) and anode double layer capacitance (C_{dl}) of LFFC at various anode flow rates

Both Figures 4.1 and 4.2 demonstrate that, as the flow rate increases, the onset potential and $R_{anode,ct}$ of methanol oxidation increases. Thus, it is harder to oxidize the methanol at the anode electrode with the higher methanol flow rate, which leads to the lower anode current output.

The change in $R_{anode,ct}$ with a lack of change in R_{ele} would indicate that the flow rate effect occurs at the electrode solution interface. From the electroneutrality condition it is easy to deduce that a fluid with zero charge density can have no effect on the ionic current in the solution [48]. Therefore, in the bulk fluid, where the electroneutrality condition applies, there should not be any effect of flow rate on the conduction of protons across the cell. This is shown by the constant R_{ele}. However, at the solution-electrode interface, where the solution is not electrically neutral, the bulk flow cannot be neglected. This region is also referred to as the electric double layer, whose structure directly impacts the electrode kinetics. The double layer is an imbalance of positive and negative ions leading to a charge density that balances out the charge in the electrode. The position of these ions is a balance between the diffusion and migration driving forces on the ions [48-49]. Since these ions are in a moving solution, this balance should be affected by the bulk flow and therefore so would the structure of the double layer.

The double layer and electrode kinetics are directly related [49]. The double layer affects the local concentration of ions at the solution-electrode interface. Also, the structure of the double layer affects the potential drop that is the true activation overpotential for electrode kinetics [49]. A change in double layer structure also leads to a change in double layer capacitance. Evidence of this change in double layer is seen in Figure 4.2.B as C_{dl} decreases with increasing methanol flow rate. Because flow rate

affects the double layer structure, the electrokinetics of methanol oxidation reaction should be also influenced by its flow rates.

4.2 Methanol Flow Rate Effect in Presence of H_2SO_4 on Methanol Oxidation Kinetics

To understand the extent of the affect of the methanol flow rate on oxidation kinetics, it is imperative to study it with a fuel solution that has strong electrolyte properties. Figure 4.3 shows the anode polarization of methanol oxidation in the presence of sulfuric acid at different flow rates.

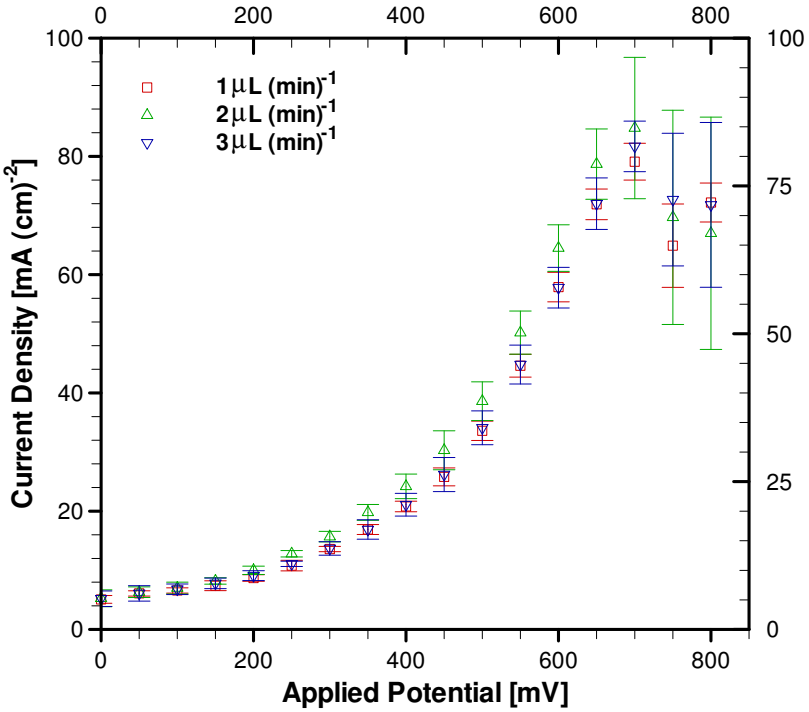

Figure 4.3 Anode Polarization of the Laminar Flow Fuel Cell Operating at 1, 2 and 3 µL/min Flow Rates. 1M methanol solution with 0.5 M sulfuric acid was fed to the anode

According to Figure 4.3, both the onset potential and anode current output of methanol oxidation reaction are not significantly influenced by the methanol flow rate.

Regardless of the methanol flow rate, with the presence of sulfuric acid in the fuel solution, the anode polarization plots are about the same. This would indicate that there is no change in anode overpotentials based on the flow rate of methanol with strong supporting electrolyte.

The impedance data also shows that there is no trend associated with the flow rate of methanol with strong supporting electrolyte. Figure 4.4.A shows the anode electrochemical impedance spectra using the various flow rates of methanol in the presence of 0.5M sulfuric acid. The Nyquist curves (impedance measurement) are essentially identical. To be thorough, the curves were fit to the equivalent circuit model. Figure 4.4.B shows that the methanol flow rate does not influence its $R_{anode,ct}$ significantly.

This tendency, seen in Figures 4.3 and 4.4, indicate that the addition of sulfuric acid in the anode fuel stream can eliminate the negative effect of high methanol flow rates. Figure 4.4.B also shows that the C_{dl} is essentially unchanged at different methanol flow rates. This means that the double layer structure is no longer affected by the bulk flow of the solution. It is known that the addition of an excellent electrolyte, such as 0.5M sulfuric acid, decreases the width of the double layer dramatically, on the order of 1 nm [48]. It should also be noted that due to the no slip condition, the bulk fluid velocity decreases to zero at the electrode interface. We speculate that this extremely narrow width of the double layer region of solution is too close to the electrode surface to be substantially affected by the bulk flow. As a result, the anode performance and methanol oxidation kinetics of LFFC are not significantly affected by the high methanol flow rate if sulfuric acid is present in the solution.

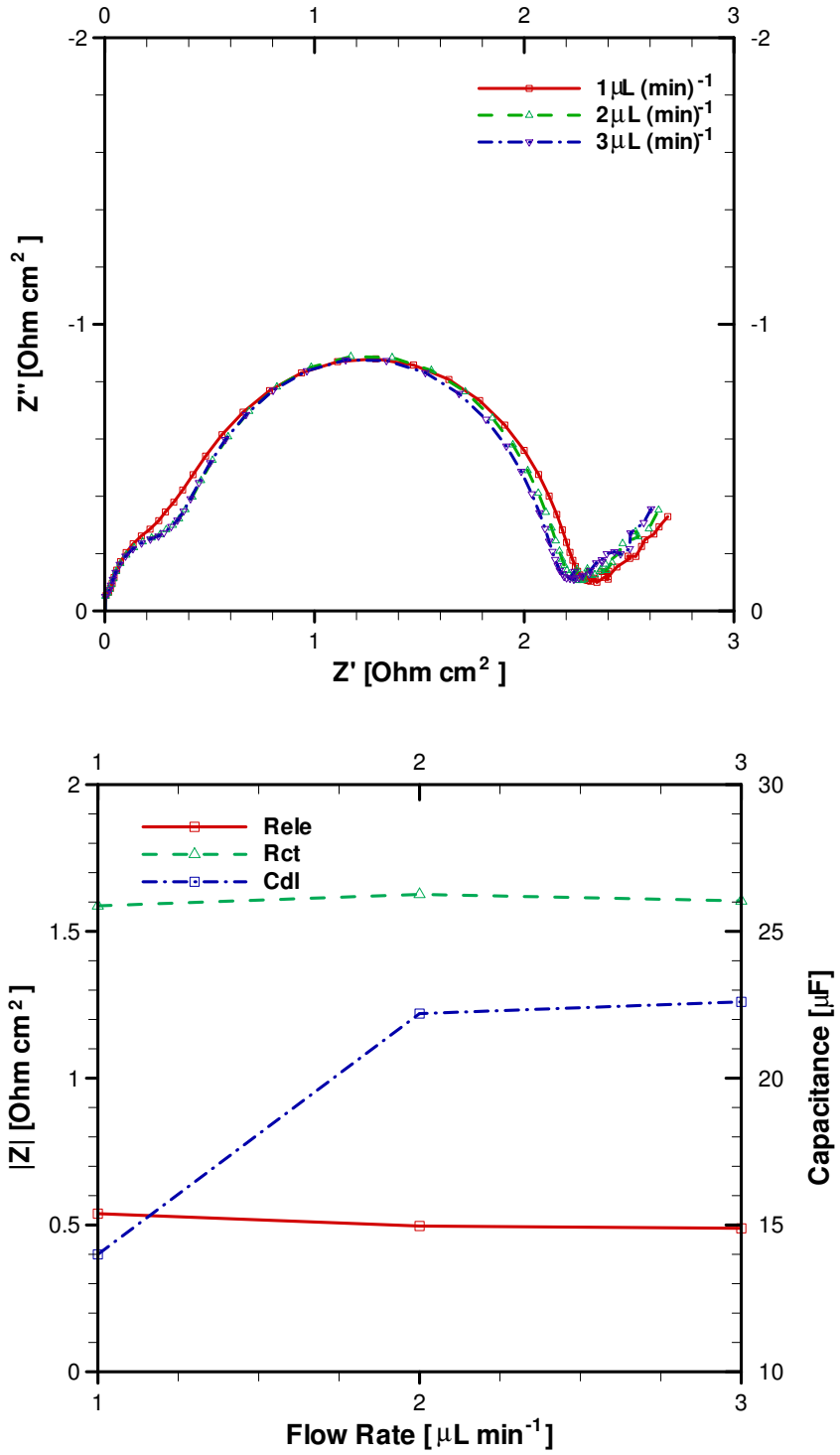

Figure 4.4 (A) Anode Impedance spectra showing the methanol flow rate effect in the presence of sulfuric acid. Methanol concentration was fixed at 1M in 0.05M sulfuric acid solution. (B) The equivalent circuit fit values of solution resistance (R_{ele}), anode charge transfer resistance (R_{ct}) and anode double layer capacitance (C_{dl})

4.3 Effect of Concentration of H_2SO_4 on Methanol Oxidation Kinetics

Clearly the electrolyte strength of the fuel stream is important to the anode performance of LFFC's. Figure 4.5 shows a direct comparison of the anode polarization data at 2 µL/min. According to the data, the addition of sulfuric acid to the methanol solution decreases the onset potential of methanol oxidation by 200 mV, and increase the anode current output over the entire applied anode potential range that we have studied.

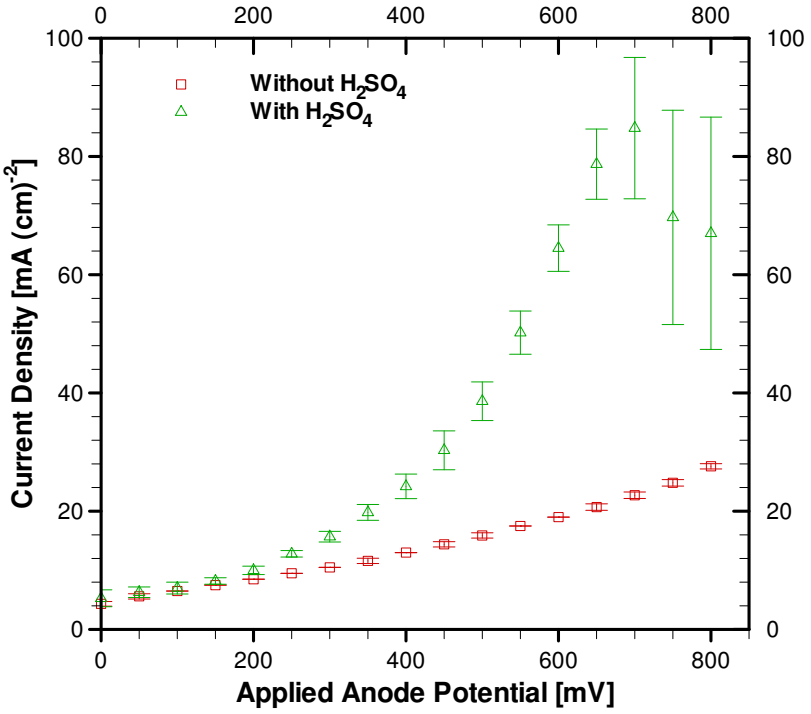

Figure 4.5 Anode polarization curves for with 0.5 M sulfuric acid added to the fuel solution and without. The concentration of methanol was fixed at 1M and the flow rate at 2 µL/min.

The effect of sulfuric acid concentration on the anode impedance is shown in Figure 4.6. Figure 4.6.A shows the impedance data with different concentrations of sulfuric acid at 2 µL/min. It can be seen that a strong electrolyte greatly reduces the overall impedance of the anode. Figure 4.6.B shows the equivalent circuit fitting results.

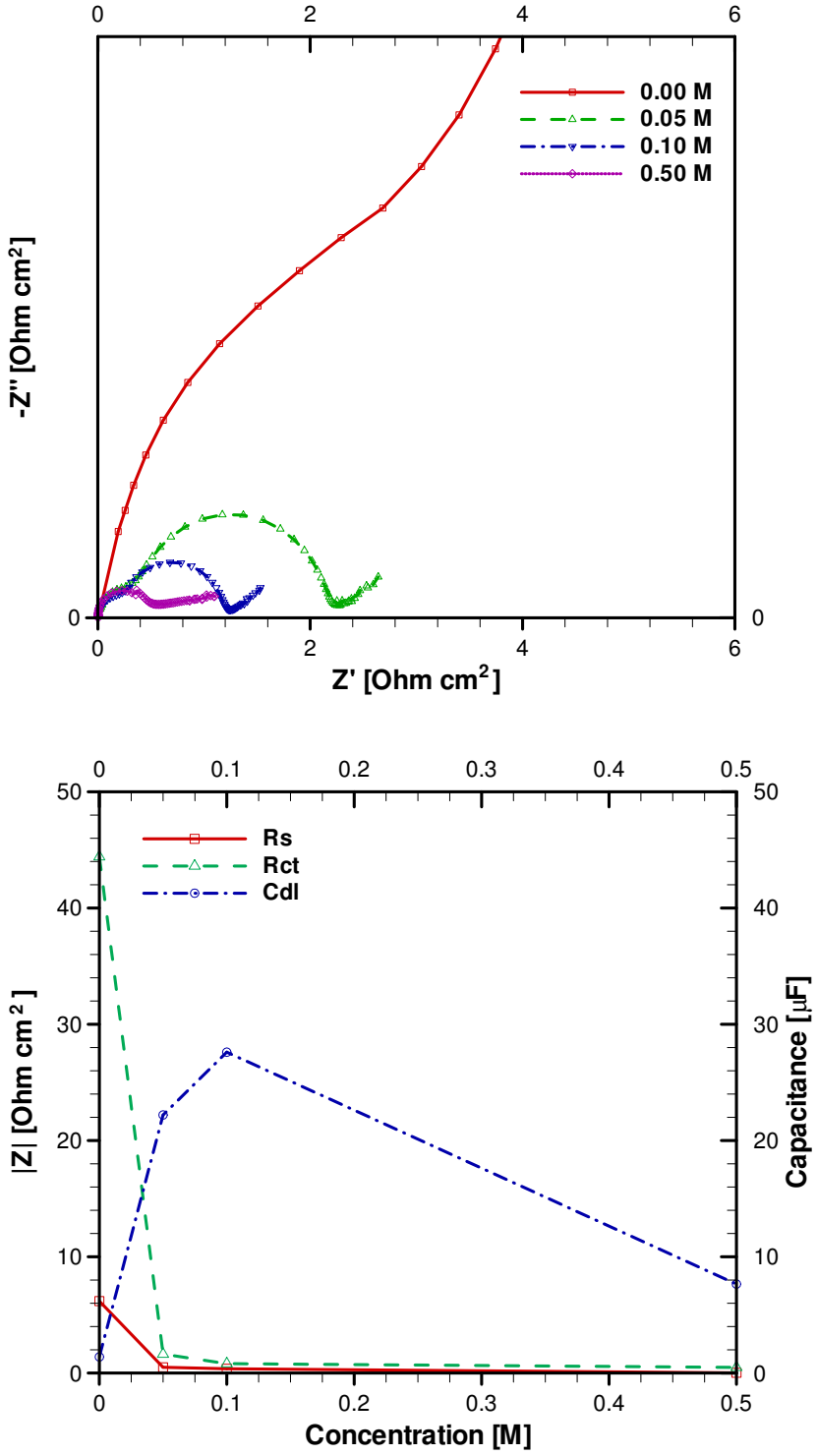

Figure 4.6 (A) Anode Impedance spectra with the various concentrations of sulfuric acid added to the fuel solution. The methanol concentration was fixed at 1M and the flow rate fixed at 2 μL/min. (B) The equivalent circuit fit values of solution resistance (R_{ele}), anode charge transfer resistance (R_{ct}) and anode double layer capacitance (C_{dl})

In this case, both the R_{ele} and $R_{andoe,ct}$ drastically decrease with increasing sulfuric acid concentration. The value of C_{dl} also increases as the electrolyte concentration increases from 0 to 0.1M, which is in accordance with well known double layer theory. However, as the electrolyte concentration increases furthermore from 0.1 to 0.5M, the value of C_{dl} decreases, and would appear to be an anomaly. We speculate that this value of C_{dl} at the 0.5M sulfuric acid is probably not accurate because the anode operating with a strong electrolyte becomes mass transport limited (This point is discussed in more detail in the next section). Thus, neglecting the Warburg impedance in this situation is not a good assumption. The change in R_{ele} makes sense because the solution resistance to conduction of protons should decrease significantly in the presence of a good ionic conductor. Adding sulfuric acid to the anode can influence its kinetic both positively and negatively. Based on the previous methanol oxidation studies using the conventional three electrodes electrochemical cell, the presence of sulfonic anion (SO_4^{2-}) negatively affects its electrokinetics by strongly adsorbing to the active sites of electrode [50]. The presence of sulfuric acid can positively affect the electrokinetic of methanol oxidation by improving its proton conduction. For our LFFC, we believe that the positive effect of sulfuric acid is more dominant over its negative effect on the methanol oxidation kinetics. Thus, its anode charge transfer decreases with higher concentration of sulfuric acid in the anode stream.

4.4 Diffusion Limited Conditions

It was stated in the equivalent circuit section that the performance in this study was generally not diffusion limited. However, in the case of 0.5M sulfuric acid in the fuel stream, there was evidence of mass transport limitations at high loads. The anode

polarizations in Figure 4.3 show that in the presence of sulfuric acid the anode performance peaks at 700 mV and beyond that becomes mass transport limited. The impedance spectra will also show diffusion transport limitations in the form of the Warburg impedance. This Warburg impedance is present as a straight line in the low frequency region, right side of the Nyquist plots. Ideally it is at an angle of 45 degrees, although this is not always observed. This is most clearly seen in Figure 4.5.B that shows different impedance spectra for different concentrations of sulfuric acid in the methanol. For the case with 0.5 M sulfuric acid, the semi circle breaks off into a linear line at a much higher frequency then in the case of 0.1M or 0.05M sulfuric acid. According to Figure 4.2.A, impedance data without sulfuric acid shows only a small linear line at the very end of the spectrum. This data shows that, as the kinetic limitations are reduced by the presence of sulfuric acid in the fuel solution, the anode then becomes more mass transport limited.

CHAPTER 5

Electrochemical Impedance Spectroscopy

5.1 EIS View of Experimental Observations

The device characterization Chapter 3 presented some interesting performance trends. A strong negative impact of increasing methanol concentration on performance and long term instability were both demonstrated. However not many conclusions could be drawn from the data and it was left for further investigation. To take a closer look at these findings electrochemical impedance spectroscopy was used and the results presented in this chapter. Electrochemical impedance spectroscopy is a powerful technique that can be applied for in situ characterization of the different performance limitations in a fuel cell. Things like electrode kinetics and solution resistance can be directly studied, allowing for a deeper understanding of what is happening in the cell.

5.2 Optimizing the Experimental Parameters

Before any experiment for scientific inquiry could be performed it was first essential to optimize the experimental parameters. Electrochemical impedance spectroscopy works by supplying an alternating signal to the cell and measuring its response. The signal can either be a controlled potential input and a measured current response, potentiostatic, or a controlled current input and a measured potential response, galvanostatic. For studying fuel cells it is generally considered that potentiostatic is more accurate and therefore this approach was used here [45]. The parameters for the input signal are the AC amplitude and the DC offset. The AC amplitude is important because

the signal needs to large enough that a measurable change in the response will occur but not so large that the response no longer remains linear. To find this amplitude an amplitude sweep was done to see what was the optimal amplitude for this device. An amplitude of 50 mV was determined to be the appropriate input for this study.

The DC offset corresponds to a load applied to the fuel cell. No offset would mean that the device is being studied at open circuit potential. Applying an offset means that the fuel cell is being studied when producing current. Initially a DC offset sweep can be performed at a constant frequency to find the range in which the cell provides a meaningful response. For the LFFC studied here it was found that an offset between 0 mV and 200 mV would provide good data. It is important to consider various offsets because the behavior of impedance in a fuel cell can change with varying amounts of current draw. Therefore all impedance spectra were taken at three loads, open circuit, 100 mV offset, and a 200 mV offset. Figure 5.1 shows impedance spectra for these three loads for the LFFC supplied with 1 M methanol at a flow rate of 2 μL/min. It can be seen that the impedance of the LFFC did not change much with increased current draw. In fact, the open circuit and 100 mV case are nearly identical and the 200 mV case shows only slightly lower impedance. It is interesting to note that the 200 mV spectrum is identical to the others in the high frequency region of the impedance plot. It only diverges in the frequency ranges associated with electrode kinetics. This would imply that the higher load has more efficient kinetics. This would make sense because the kinetic relationship with load is exponential so at an electrode potential further from open circuit the increase in current is greater. If the three different loads are compared at each set of operating conditions the trend is essentially identical to that showed in Figure 5.1. Therefore all

other impedance data presented is only presented for the open circuit case.

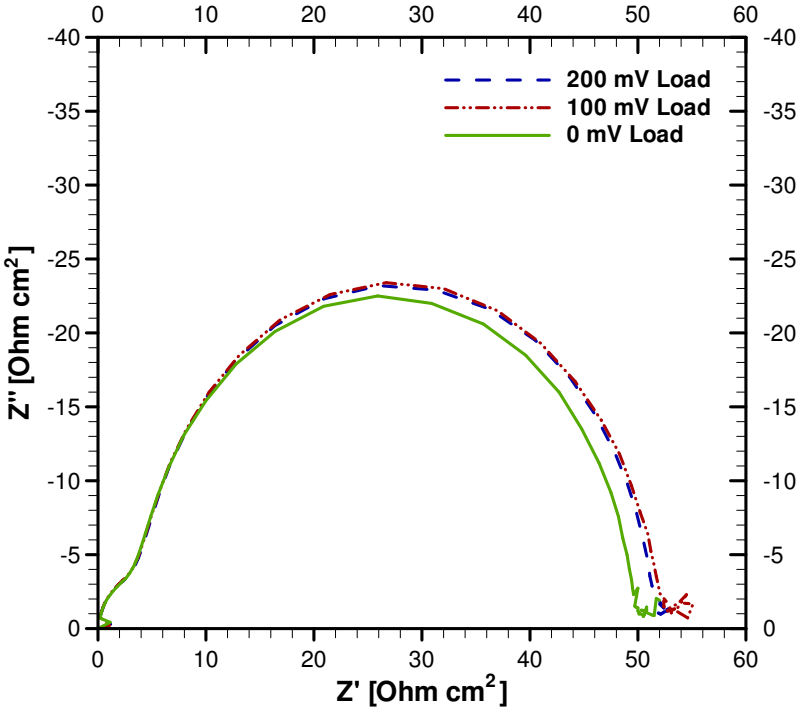

Figure 5.1 Impedance Spectra for Different DC Offsets for a LFFC Operating with 1 M methanol fuel solution flowing at 2 µL/min

5.3 Stability

Stability was broken down into two types for the purpose of study with electrochemical impedance spectroscopy, short term stability and long term stability. Short term stability was used to check the validity of impedance spectroscopy results. Essentially, impedance was measured as a function of time at a constant frequency. Figure 5.2 shows 10 minutes of data taken at 1000 Hz for the various loads with a 50 mV amplitude.

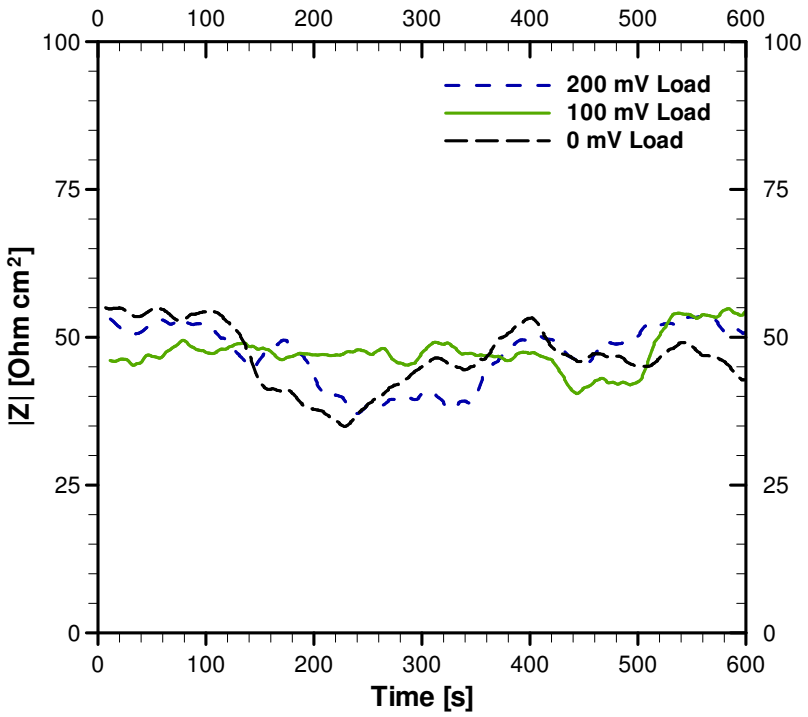

Figure 5.2 Impedance Measurement of Short Term Stability for different DC Offsets. The input signal had a constant frequency of 1000 Hz and amplitude of 50 mV. The anode was fed 1 M Methanol at 2 µL/min

It can be seen that there is some level of short-term instability in the LFFC; this was even witnessed to some degree in the performance characterization presented in an earlier chapter. There is however no noticeable trend associated with load. Based on these results it was decided that for each set of operating parameters four impedance spectra would be taken over a period of 10 minutes and averaged for the final result. By taking the average the short term stability could be made negligible giving credence to the observed trends.

Long-term stability is the same as presented in Chapter 3. To study the long term behavior the device was operated at open circuit for a period of 48 hours and the impedance was measured at three times throughout. Figure 5.3 shows impedance spectra

for 4, 24, and 48 hours after operation.

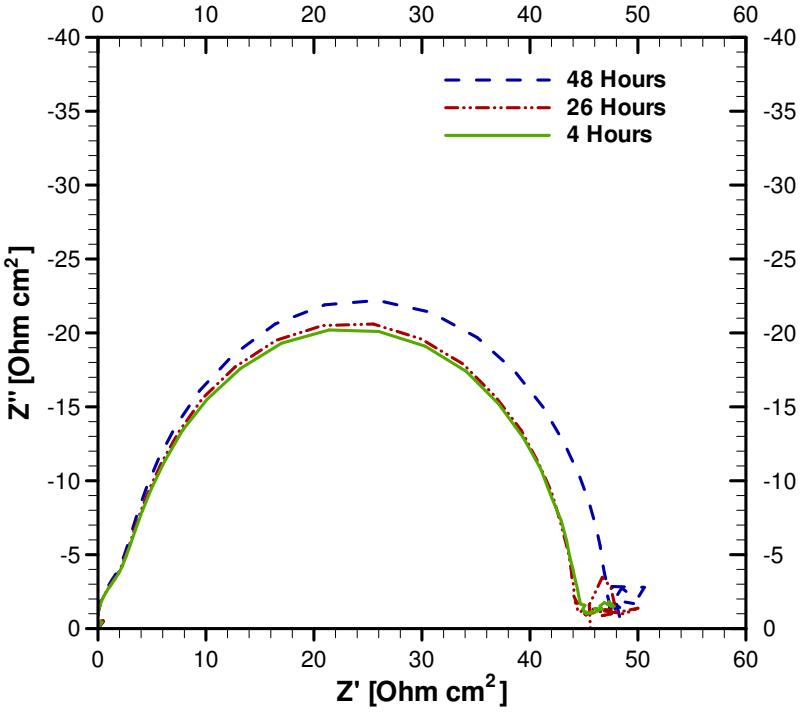

Figure 5.3 Impedance Spectra taken at different times from a continuously operated device. The anode was fed 1 M methanol at 2 µL/min for a period of 48 hours.

There is not a significant change in impedance over time. It is not too surprising that an impedance analysis did not provide further insight into the long-term stability because the change measured was in open circuit potential which is not a function of impedance.

5.4 Anode versus Cathode

The bulk of the work presented in this thesis studies the anode performance for a direct methanol LFFC. It is important, then, to know how the anode performance fits in with the overall device performance, especially when previous works have cited the cathode as the dominant limitation for LFFC's [4]. Figure 5.4 shows measured impedance

comparisons between the anode and the cathode at various flow rates. For the purpose of direct comparison both electrodes were supplied with the same concentration of a strong supporting electrolyte, 0.5 M sulfuric acid. In the device studied in this work the limitations for the anode and the cathode were comparable with the anode being slightly worse for flow rates of 2 and 3 µL/min. Only at the slower flow rate does the cathode impedance appear to be slightly higher.

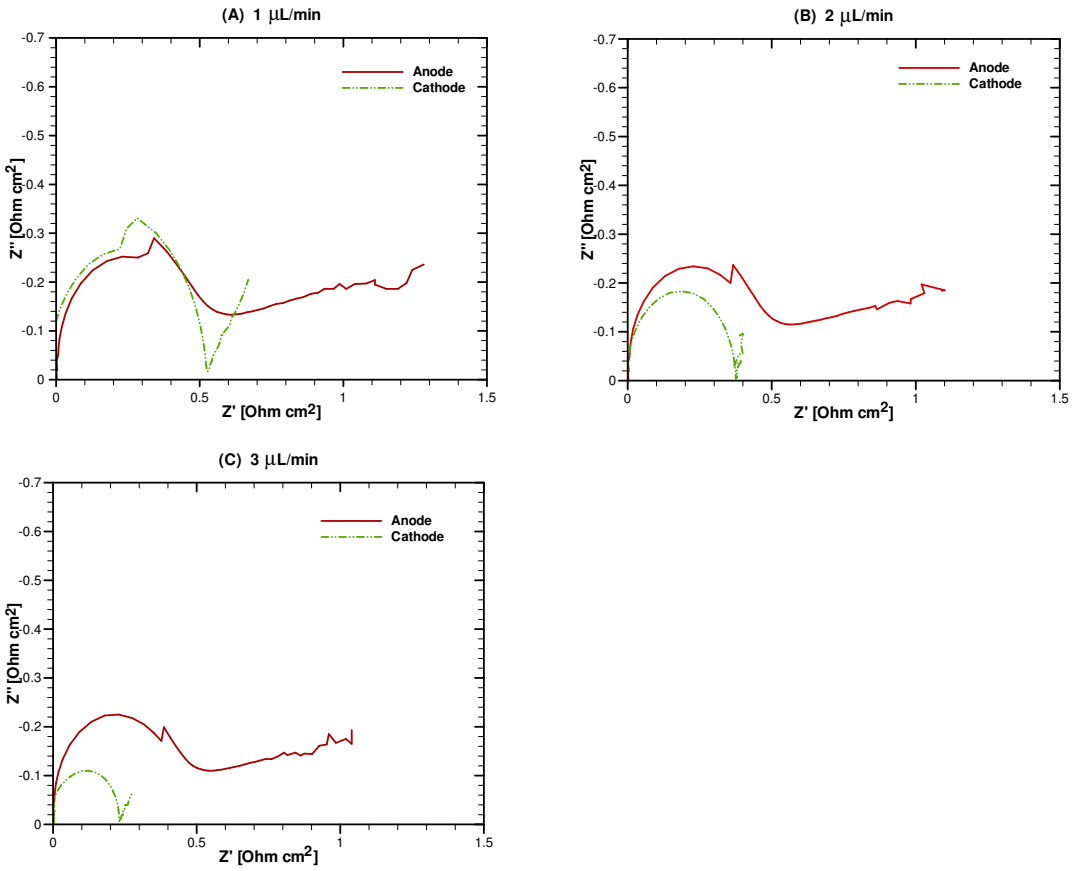

Figure 5.4 Impedance Spectroscopy Analysis comparing the anode and cathode limitations for (A) 1 µL/min, (B) 2 µL/min, and (C) 3 µL/min. The anode was tested with 1 M methanol and 0.5 M sulfuric acid solution. The cathode was tested with oxygen saturated 0.5 M sulfuric acid solution.

An interesting observation from Figure 5.4 is that the cathode impedance is a strong function of reactant flow rate, as flow rate increases the cathode impedance

decreases. This is an expected result because it has been shown that the cathode of a LFFC is transport limited [4,37]. This is because oxygen cannot be dissolved in an aqueous solution to a high concentration. So the oxygen at the electrode gets depleted quickly and isn't replenished quickly enough. A higher flow rate will replenish the oxygen to the electrode better and therefore the impedance will decrease. Evidence of the transport limitations shows up in Figure 5.4 in the form of Warburg impedance. There is also evidence in Figure 5.4 that the cathode kinetics is less efficient at a lower flow rate. This is likely due to the fact that the reactants are not evacuated as efficiently and the will therefore hinder the reduction reaction.

The anode impedance plots do not change much for each of the flow rates. This is because as discussed before the addition of a supporting electrolyte reduces or eliminates the flow rate effect on the methanol oxidation. The impedance does not decrease like it does for the cathode, however, because there is no benefit for the oxidation reaction to having an increased methanol concentration for concentrations this high. If the methanol supplied was on the order of mM then perhaps there would be, but because the bulk fluid concentration is 1 M the electrode already has as much methanol as it can handle. However, without the supporting electrolyte in the anode, as is the case for a lot of the results presented in this work, the anode limitations are far greater and the cell is anode limited.

5.5 Methanol Concentration Effect

The performance characterization showed that with increasing methanol concentration in the fuel stream the device performance decreased dramatically. Figure 5.5 shows impedance spectra of the methanol effect at different flow rates. It can be seen

that the methanol concentration effect is independent of flow rate. Figure 5.5.D shows the results from the equivalent circuit analysis for a flow rate of 3 µL/min.

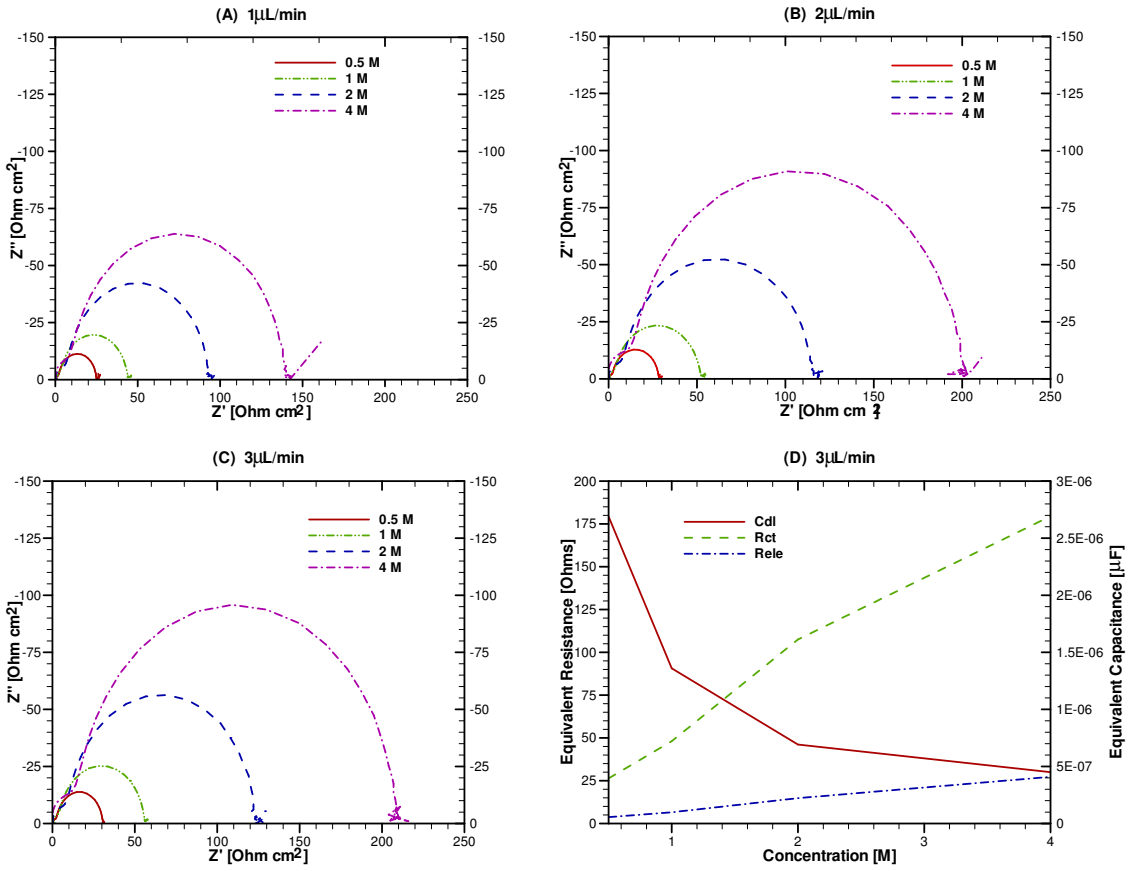

Figure 5.5 Impedance Spectra and Equivalent Circuit Analysis for the Methanol Concentration Effect at various flow rates

As expected, R_{ele} increases with increasing methanol concentration. This is because protons have a lower mobility in an aqueous solution with higher concentrations of methanol; therefore the bulk solution has lower proton conductivity or a higher electrolyte resistance. R_{ct} also increases with increasing methanol concentration. This implies that the methanol oxidation kinetics is worse with a higher concentration of methanol. This is likely due to a change in the electric double layer with different methanol concentrations. As stated previously the double layer affects kinetics in two

ways, first the concentration of ions at the plane of closest approach and through its structure. Methanol is a neutral ion and its concentration at the plane of closet approach wouldn't be altered by the electric double. Also, a higher concentration of methanol in the bulk fluid should result in a higher concentration of methanol at the plane of closest approach that is where the kinetic reaction is occurring. Therefore, the trend in kinetics associated with methanol concentration is likely due to a change in the double layer structure. The observed C_{dl} supports this conclusion because it decreases with increasing methanol concentration. A lower C_{dl} equates to a wider electric double layer which would mean worse kinetics. Therefore the negative reaction order of methanol oxidation displayed in the LFFC is directly related to the electric double layer structure.

5.6 Flow Rate Effect

The flow rate effect was presented in great detail in chapter 4. It is included again here to show that it is present regardless of the concentration of methanol used in the fuel solution. Figure 5.6 shows impedance spectra comparisons of the different flow rates at different methanol concentrations. Figure 5.6.D shows the results from the equivalent circuit analysis for 2 M methanol.

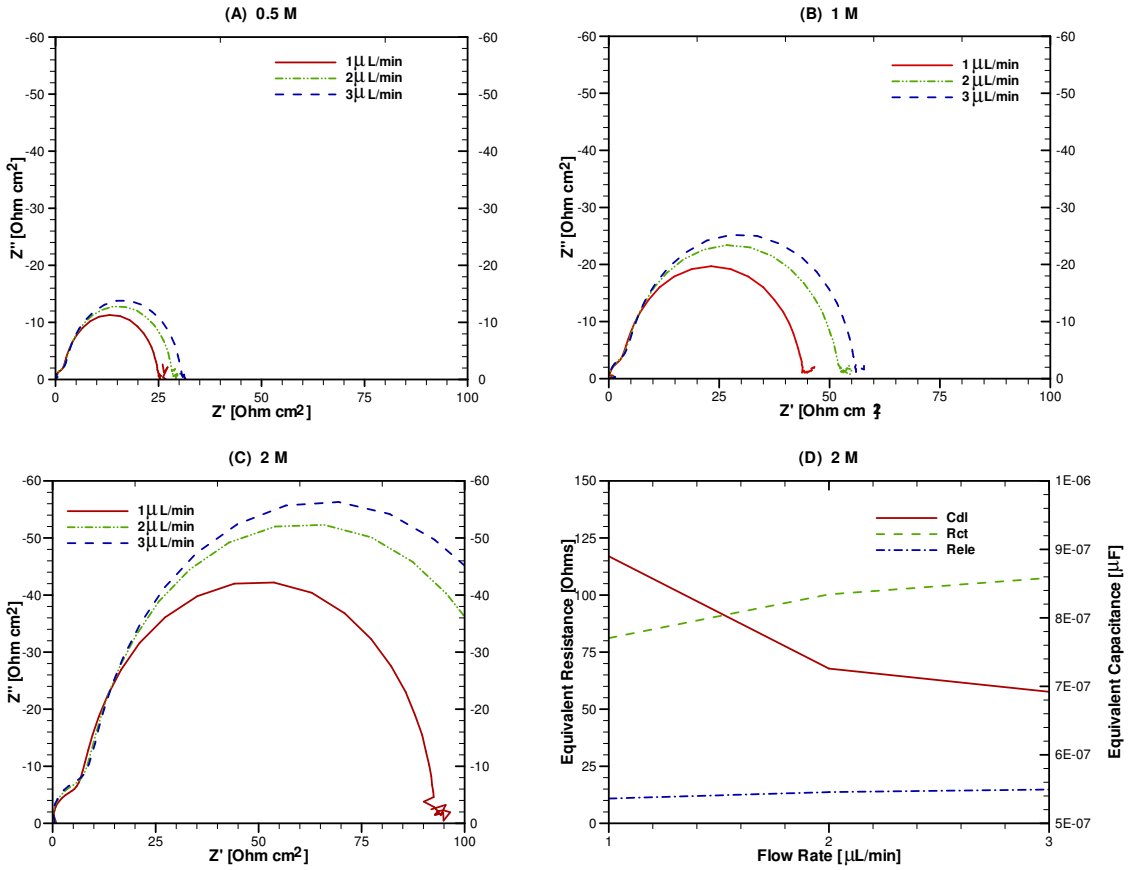

Figure 5.6 Impedance Spectra and Equivalent Circuit Analysis for the Electrolyte Flow Rate Effect at various methanol concentrations

There is no change in the effect at different concentrations and the conclusions about the impact of the electrolyte flow rate remain the same.

5.7 Channel Size

The width of the channel studied is relatively large. This was done to aid in fabrication and isolating the anode performance. However, it is critical to study the observed phenomena in a narrower channel to see how the trends may change. Figure 5.7 shows the methanol concentration and flow rate effect at two different channel widths.

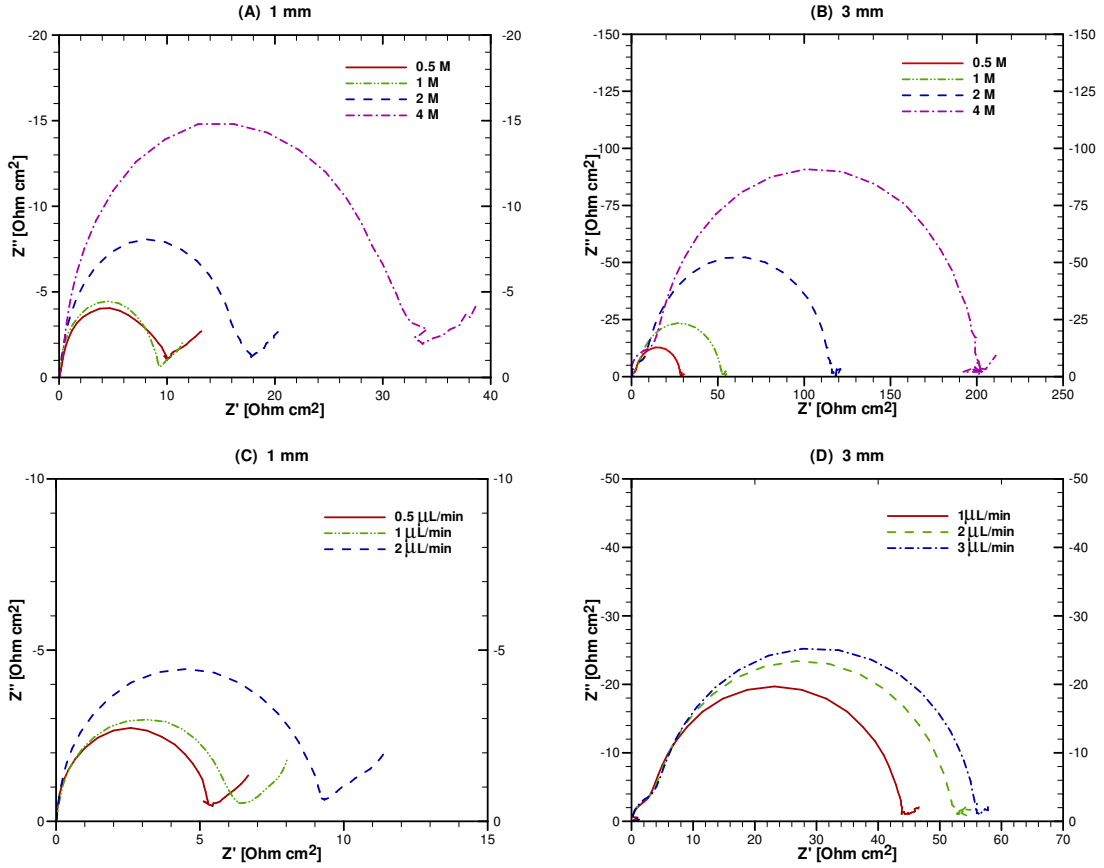

Figure 5.7 Impedance Spectra for the Methanol Concentration Effect and Electrolyte Flow Rate Effect in two different channel widths

The first thing to notice is that the overall scale of impedance is significantly less. This is expected because the performance of any fuel cell is greatly decreased the further apart the electrodes are. However, the trends remain essentially the same. This means that the results presented in this work are of importance to LFFC design in general and are not just an artifact of the large device width. Figure 5.8 shows the results for the equivalent circuit analysis for the four cases in Figure 5.7.

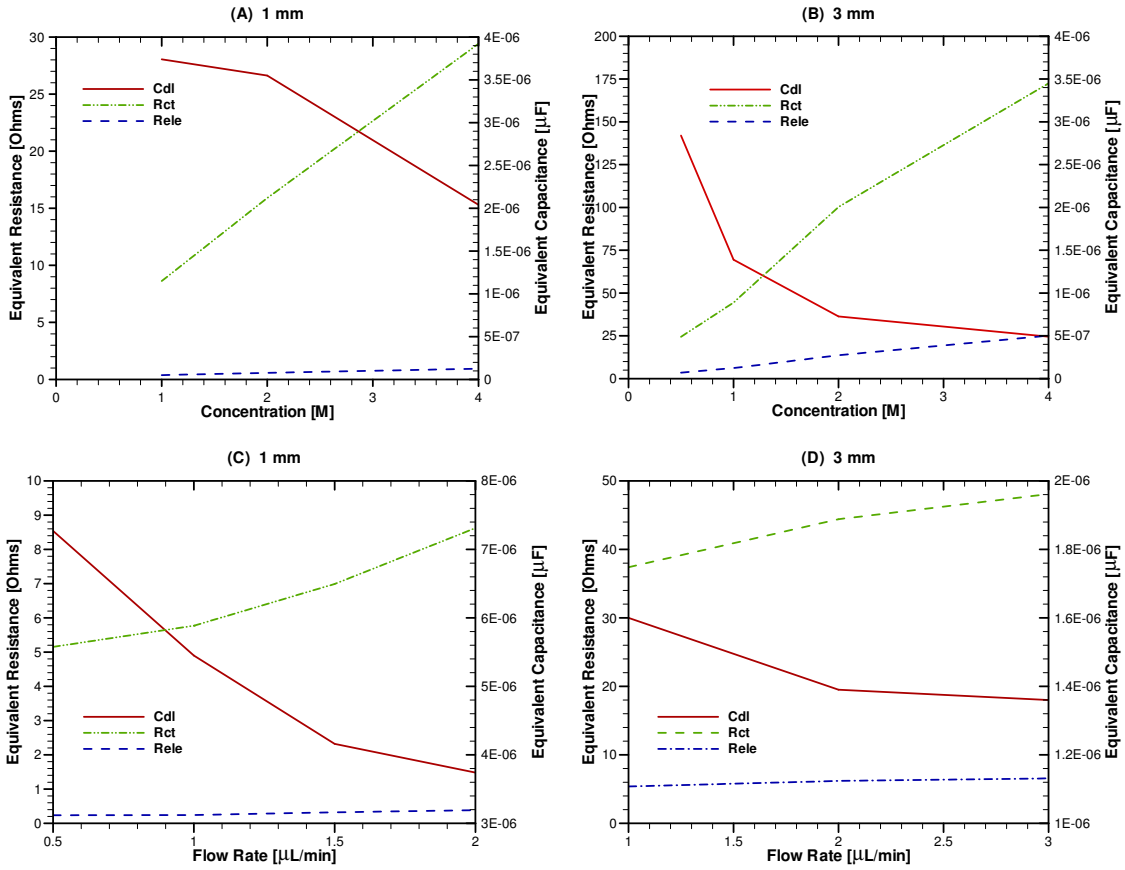

Figure 5.8 Equivalent Circuit Analysis for the Methanol Concentration Effect and Electrolyte Flow Rate Effect in two different channel widths

It can be seen that R_{ct} still increases with increasing flow rate or concentration and C_{dl} still decreases. This would indicate that the trends are still related to the electric double layer structure. Therefore, because the effects of methanol concentration and electrolyte flow rate are due to the microscopic interfacial effects they are still present in the smaller channel.

CHAPTER 6

Mathematical Model

6.1 Computational Domain

The scope of the analytical work presented here is to show a mathematical model that will demonstrate cell behavior analogous to what was observed in experiment. A system similar to the LFFC characterized experimentally is considered. The bulk fluid velocity for the laminar flow is solved separately and for a device of similar design to the experimental LFFC. However, because the microscopic interfacial phenomenon is the critical focus of this model only a small region at the start of the anode electrode is used for the computational domain for the electrochemical model as shown in Figure 6.1. Since a continuum mechanic approach is only valid for the diffuse double layer the domain starts, $y = y_{OHP}$, at the Outer Helmholtz Plane. To ensure the entire interfacial behavior is captured the domain extends out into the bulk solution, $y = y_{max}$, where the solution is known to be electrically neutral. The domain is at the start of the anode to capture the development of the electrical double layer as the bulk fluid entering the channel, $x = 0$, comes into contact with the electrode. By the end of the domain, $x = x_{max}$, the electrochemical effects are fully developed.

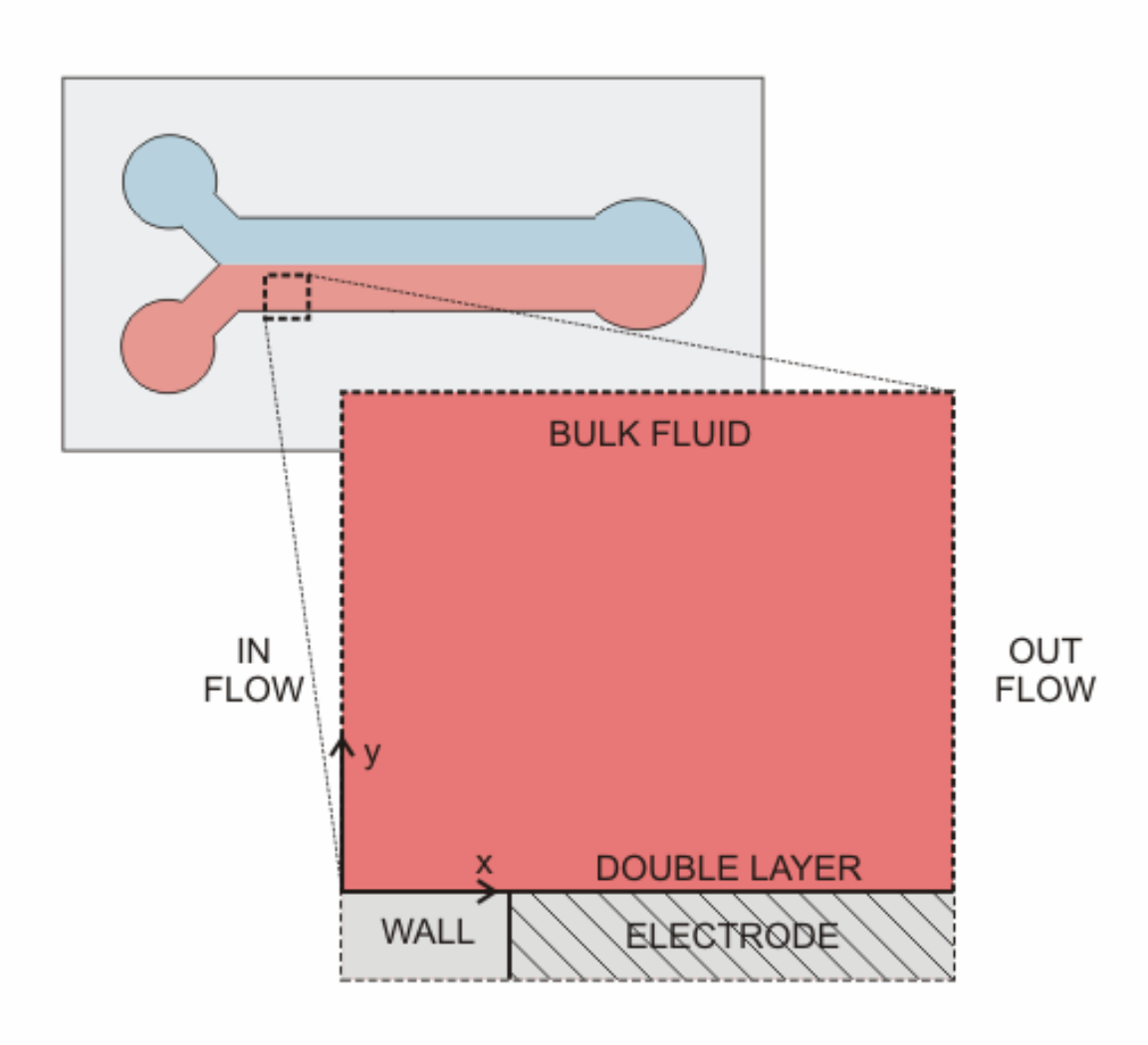

Figure 6.1 The Computational Domain Considered in the LFFC Model

6.2 Governing Equations

It is assumed that the electrochemical system is steady state and the streams are an incompressible flow. Therefore the governing equations are well known and are simply the steady state Navier-Stokes equations

$$\nabla \cdot (\rho \vec{v} \vec{v}) = \nabla \cdot (\mu \nabla \vec{v}) - \nabla P \tag{6.1}$$

and the steady state continuity equation:

$$\nabla \cdot (\rho \vec{v}) = 0 \tag{6.2}$$

Where ρ is the density of the anode solution, $\vec{v}$ is the velocity field, μ is the dynamic viscosity, and P is the pressure. These equations were used to obtain the velocity field for the entire channel and then the results for the computational domain were extracted and used in the main electrochemical model.

For the model the electrochemical reaction considered was a general oxidation equation that will show behavior similar to the methanol oxidation presented prior to now. This takes the form of

$$D \leftrightarrow A^+ + e^- \tag{6.3}$$

Where A^+ is the oxidized species, for example protons, and D is the reduced species, which would be methanol. These species are dissolved into an aqueous solution along with a supporting electrolyte. The electrolyte is a binary electrolyte consisting of the charged A^+ ions and a counter ion of negative charge, this could be OH^- for example. The transport of these ions in the solution is governed by a species balance that takes the form of

$$\nabla \cdot (\vec{v} C_i) = \nabla \cdot (RT\omega_i \nabla C_i + z_i \omega_i F C_i \nabla \phi) \tag{6.4}$$

Where the subscript *i* refers to each species in the simulation, OH^-, protons, and methanol, and ω_i is the mobility, z_i is the charge, and C_i is the concentration all of the i^{th} species. Also R is the universal gas constant, T is the absolute temperature, F is the Faraday constant, and ϕ is the potential in the solution. The left side of the species balance represents species transport due to advective effects, or the bulk flow of the solution. The right side has two parts, the first is diffusion that is driven by the concentration gradient and the latter is the transport from a charged ion in an electric field, known as

electromigration. In many previous fuel cell models the electromigration term has been neglected because the charge carrying ions are not accounted for in the model. Also, the electrode-solution interface, where the solution is not electrically neutral, has been neglected. In this study these are of paramount importance. Because the electrically charged interface region and the charge carrying ions are to be included in this work the typical charge balance equation cannot be used to describe the potential distribution in the solution. Instead a more fundamental equation must be used, a Poisson's equation for electrostatic potential.

$$-\nabla \cdot (\varepsilon \varepsilon_0 \nabla \phi) = F \sum z_i C_i \tag{6.5}$$

ε is the relative static permittivity and ε_0 is the permittivity in vacuum. The right side of this equation is the charge density. Charge density will be zero when the ion concentrations are balanced, such as in the bulk flow, but will begin to have magnitude in the interface region because of the electric double layer effects.

Although Poisson's equation is not often used for fuel cell type modeling it has been studied for generalized electrochemical systems to study the double layer. However, in these previous works the advective term of the species balance has been neglected. Due to the nature of this problem, it is important to include this to see if any of the experimental flow effects can be shown analytically.

6.3 Boundary Conditions

Because the compact layer cannot be modeled using continuum level theory and the generation and consumption of species due to the electrode kinetics occurs as the Outer Helmholtz Plane the compact layer and the electrode kinetics are accounted for in the boundary conditions. The stern model provides the link between the potential of the

solid electrode and the charge in the diffuse double layer. It assumes a linear profile across the inner double layer, now called the stern layer, where the electric field is continuous with that in the diffuse double layer. A key assumption is the absence of specific adsorption, or the tendency for anions to enter the inner layer and contact the solid electrode. This greatly changes the charge distribution across the interface and therefore the potential distribution. Although, OH^- is thought to have very low tendency to adsorb so this assumption is valid. This means that the potential in the compact double layer can be approximated by the Stern Layer Model

$$\Delta\phi_S = \frac{\varepsilon_S \varepsilon_0}{C_S} \left.\frac{\partial \phi}{\partial n}\right|_{@\ Electrode} \tag{6.6}$$

Where $\Delta\phi_S$ is the drop across the Stern Layer, ε_S is the permittivity in the stern layer, C_S is a constant inner layer capacitance and $\frac{\partial \phi}{\partial n}$ is the gradient of the potential in the solution normal to the electrode. C_S and ε_S have been estimated experimentally and have shown to a good estimation for the width of the Stern Layer. Using this model a boundary condition for ϕ can be established at the electrode

$$\phi = E + \frac{\varepsilon_S \varepsilon_0}{C_S} \frac{\partial \phi}{\partial n} \tag{6.7}$$

Where E is the electrode potential. The remaining boundary conditions for ϕ at the inlet, outlet, wall, and bulk fluid are

$$\frac{\partial \phi}{\partial x} = 0 \qquad \frac{\partial \phi}{\partial x} = 0 \qquad \frac{\partial \phi}{\partial y} = 0 \qquad \phi = 0 \tag{6.8}$$

The kinetics of a fuel cell are driven by the potential drop across the stern layer. The reaction consists of a forward oxidation reaction and a backward reduction reaction.

The oxidation reaction is thermodynamically favorable so it proceeds forward. As electrons are transferred from the methanol to the electrode the electrode begins to take on a net charge. This charge causes a change in the electrode potential which in turn hinders the oxidation reaction and promotes the reduction reaction. There is an electrode potential where the currents from the two reactions are equal and there is no net current. This is the open circuit potential. This view of electrode kinetics gives a net kinetic current that is simply the difference the oxidation and reduction currents

$$j = Fn\vec{k}C_D^{\alpha_D} e^{(1-\beta)\Delta\phi_s F/RT} - Fn\vec{k}C_A^{\alpha_A} e^{-\beta\Delta\phi_s F/RT} \tag{6.9}$$

Where j is the net kinetic current, n is the number of protons involved in the reaction, $\vec{k}$ is the oxidation rate constant, $\vec{k}$ is the reduction rate constant, C_d is the reduced species concentration and C_A is the oxidized species concentration. Since the reaction occurs at the interface these concentrations are taken at the plane of closest approach. α_A and α_D are reaction orders for the reduced and oxidized species respectively and β is the symmetry factor. From the kinetics the boundary condition at the electrode for the species balance are

$$J_i = \frac{s_i j}{nF} \tag{6.10}$$

Where J_i is the net ionic flux and s_i is the stoichiometric coefficient. This coefficient is determined from the balanced chemical reaction equation such as equation 6.3. It is negative if the species is a reactant and positive if the species is a product. The other boundary conditions for the species balance at the inlet, outlet, wall and bulk fluid are

$$C_i = C_i^0 \qquad \frac{\partial C_i}{\partial x} = 0 \qquad C_i = C_i^0 \qquad J_i = 0 \tag{6.11}$$

6.4 Numerical Scheme

The governing equations 6.1, 6.2, 6.4, and 6.5 and boundary conditions 6.7, 6.8, 6.10, and 6.11 were solved numerically. Care had to be taken in selecting a numerical scheme because the Poisson's equation is difficult to solve numerically. A finite volume formulation was chosen and the domain was discretized following the technique as laid out by Patankar [51]. The finite volume method ensures that the quantities are conserved throughout the domain. By discretizing the domain into finite volumes the governing partial differential equations become a system of algebraic equations. There are several techniques for solving this system of equations; commonly the TDMA algorithm is employed. The TDMA algorithm is an iterative technique that solves the equations one piece at a time and repeats until the results converge. However, in this work TDMA was used only to solve the neutral species balance. TDMA was not suited for the remaining equations because the Poisson's equation is very nonlinear and strongly coupled with the species balance for the charged ions. For these a more robust algorithm that can solve them simultaneously is necessary. An excellent technique for solving such a system of nonlinear equations is the Newton's method. Newton's method finds the direction from an initial guess towards zero and adjusts the initial guess by some correction. The system of equations can be written as

$$f(s) = 0 \tag{6.12}$$

Where s is the value of the unknowns corresponding to the solution and

$$f \in \Re^{(i+1)B} \tag{6.13}$$

Where *i* represents each species and *B* is the total number finite volumes for each equation. If the Jacobian is given by

$$J(s) = \frac{\partial f}{\partial s} \tag{6.14}$$

Then Newton's method gives the matrix equation

$$J(s^m)\eta^m = -f(s^m) \tag{6.15}$$

Where *m* is the current iteration and η is a set of corrections for *s* such that

$$s^{m+1} = s^m + \eta^m \tag{6.16}$$

The matrix equation 6.15 is solved for η and iterated until the solution has converged to an acceptable tolerance level. When η is small *s* is the approximate solution and the values for the ion concentrations and potential distribution have been solved for. Solving equation 6.15, however, is not trivial because the Jacobian is a large sparse unsymmetric matrix so many conventional matrix equation solving algorithms cannot be used. A strong algorithm for sparse unsymmetric matrices is a preconditioned GMRES based solver. The GMRES method, or Generalize Minimal Residual method, solves the matrix equation

$$Ax = b \tag{6.17}$$

The method is an iterative method based on the Krylov subspace which is of the form

$$K_m(A, v) \equiv span\{v, Av, A^2v, ..., A^{m-1}v\} \tag{6.18}$$

. The GMRES method finds the approximate vector solution for which the Euclidean norm is minimized over the Krlyov subspace. The Euclidean norm is given by

$$\| b - Ax_k \|_2 \tag{6.19}$$

A preconditioner is often applied to the Jacobian to make the system easier to solve.

6.5 Simulation Results

The equations were solved and some results of the governing system of equations are presented here. The results are presented in nondimensional format. The potential was nondimensionalized by the electrode potential, the ion concentrations by the concentration in the bulk fluid and the distance by the channel width, y_{max}. Figure 6.2 shows the potential distribution in the computational domain.

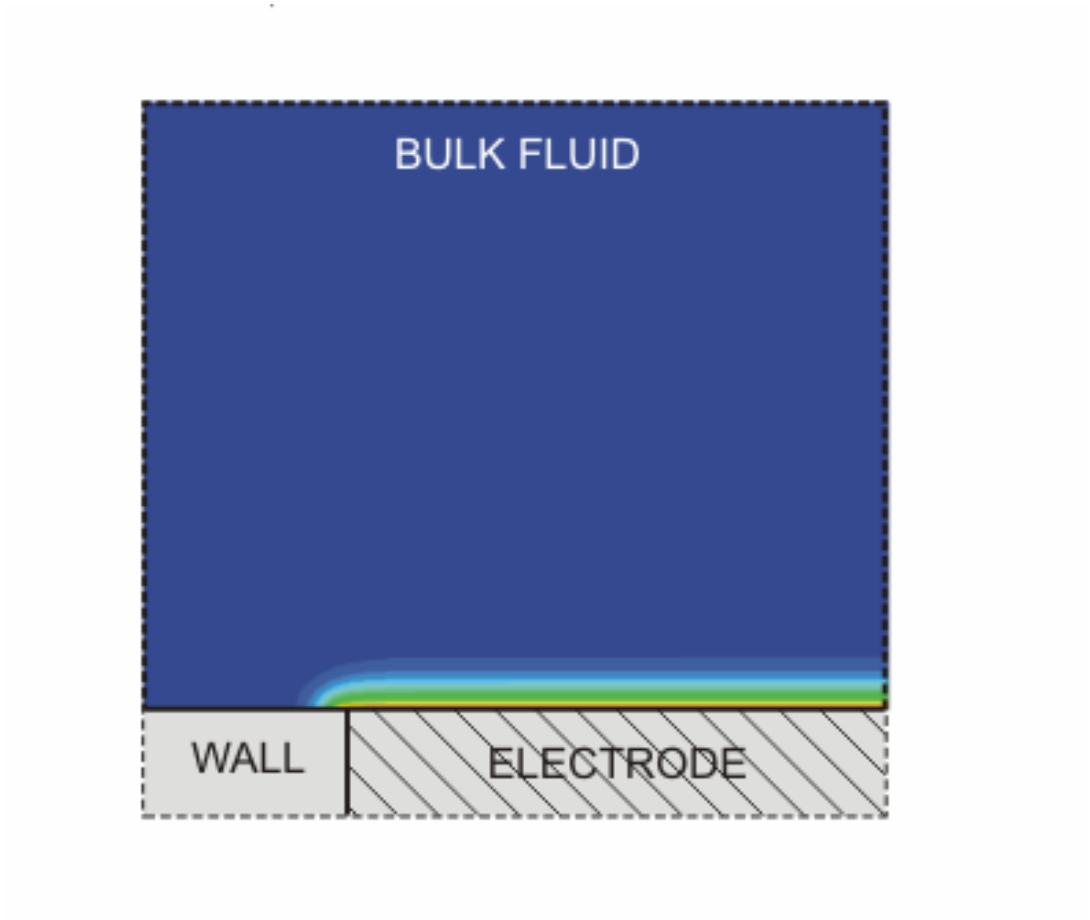

Figure 6.2 Contour Plot of the Potential Distribution in the Computational Domain

It can be seen that the information of interest lies only at the interface between the solution and the electrode. A better representation of the potential distribution can be

obtained by taking a cut across the channel and plotting the resulting data. Figure 6.3 shows such a cut for several different electrode potentials.

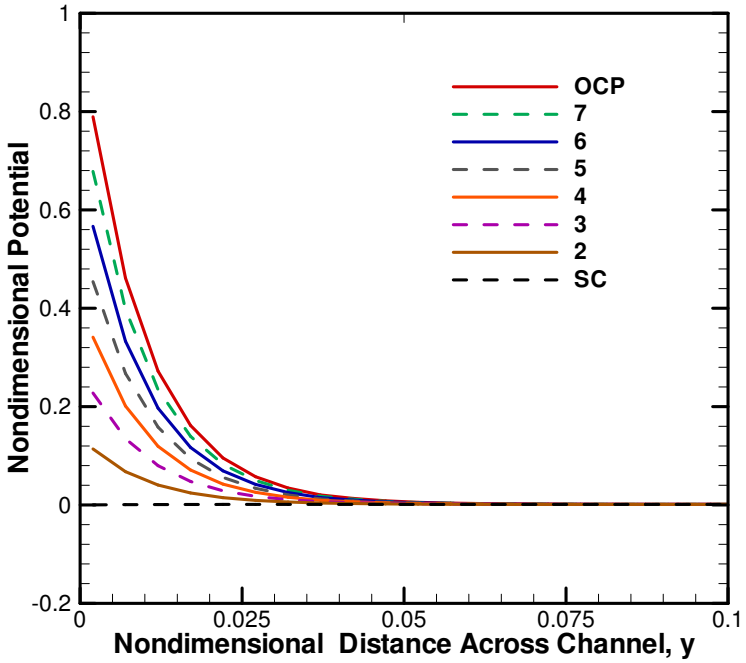

Figure 6.3 potential distributions across channel in the fully developed region for different electrode potentials

The electrode potential starts at the open circuit potential and is incrementally reduces to a short circuit, or zero potential in the electrode. It can be seen that the data doesn't start immediately at the electrode surface, but instead a small distance away. This distance corresponds to the compact double layer, and the diffuse layer starts outside of that. As assumed in the Stern Model the potential would be linear across this gap, and it is this linear drop in potential that governs the electrode kinetics. At open circuit the reduction reaction rate is equally as fast as the oxidation reaction rate and therefore no net current is produced. As the electrode potential decreases the drop across the compact layer also decreases because the slope of the potential in the diffuse layer is less steep. As

this driving force for the reaction is decreases the reduction reaction rate is becomes less than the oxidation reaction rate and therefore a net oxidation current is produce. Thus methanol is oxidized and the cell has a net current. When there is no potential difference between the electrode and the bulk solution there is no double layer formed and the cell current is at a maximum. This current corresponds to the spontaneous oxidation current that naturally happens given by thermodynamic reasons.

Key to the double layer's structure is the imbalance of ions in solution near the electrode-solution interface. This is how the charge difference between the electrode and the solution can be neutralized. Figure 6.4.A and 6.4.B show the ion concentrations at the interface at the different electrode potentials. It can be seen that far away from the electrode-solution interface both ion concentrations are equal to the bulk fluid value. Because $C^0_{H^+} = C^0_{OH^-}$ are equal the solution at this point is electrically neutral. Closer to the interface the ion concentrations begin to diverge and a charge density is developed. The sum of the charge density in the double layer will be equal but opposite to the unbalanced charge in the electrode that has caused the electrode potential. At open circuit this potential is at its greatest and at short circuit it can be seen that there is no charge density in the solution because there is no unbalanced charge in the electrode.

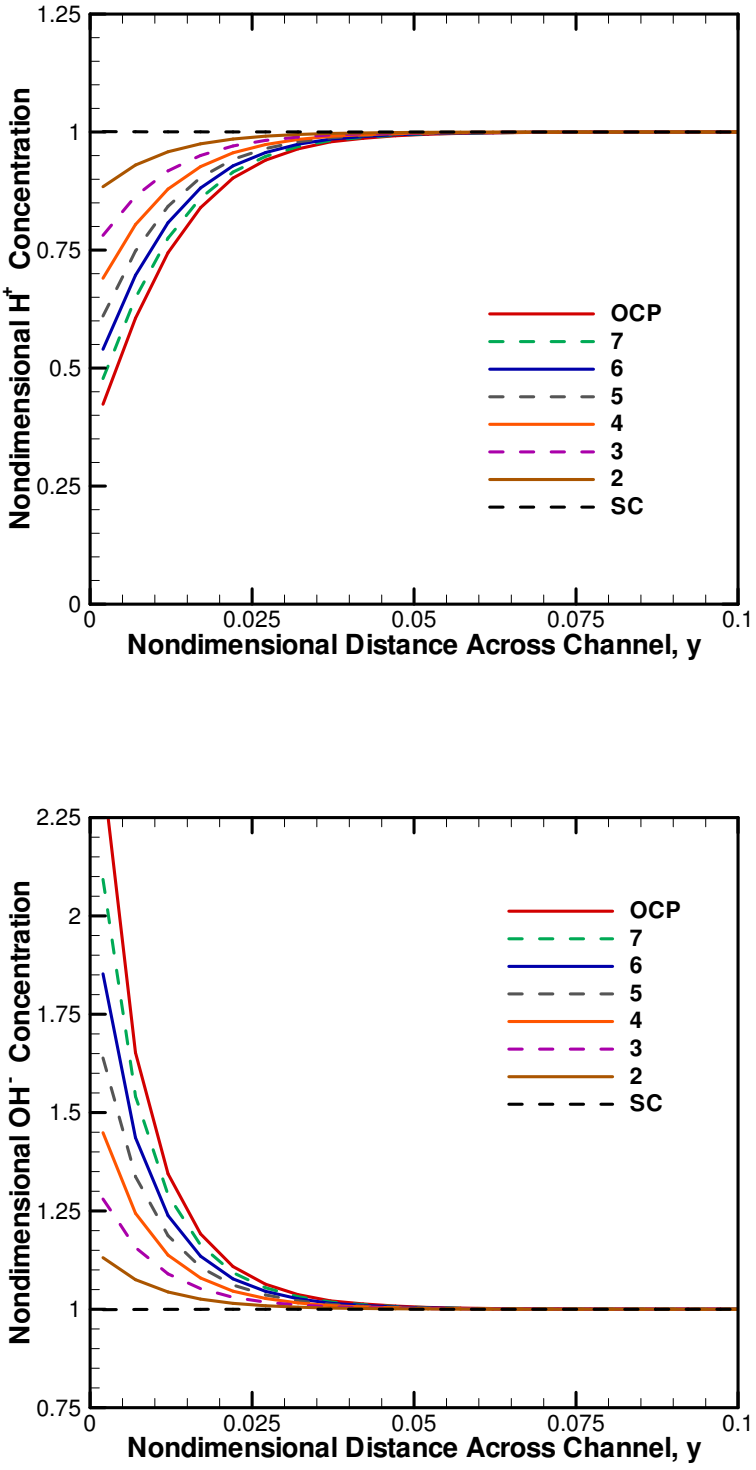

Figure 6.4 The concentration distributions across the channel in the fully developed region for (A) protons and (B) OH^- ions at different electrode potentials

Clearly, the bulk concentration of the electrolyte ions is very important to how the double layer can balance out the charge in the electrode. Figure 6.5 shows two diffuse double layer potential profiles for the same electrode potential.

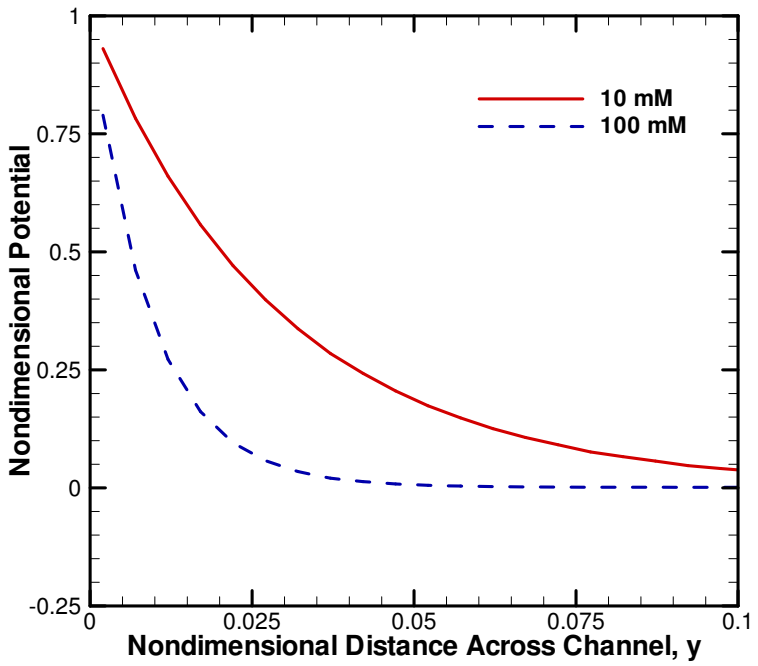

Figure 6.5 Open Circuit Potential Distributions across channel in the fully developed region for two different bulk electrolyte concentrations

It can be seen that the lower concentration of electrolyte produces a much shallower and wider potential distribution. This double layer structure difference will affect the kinetics. Figure 6.6.A and 6.6.B show performance curves for the anode at two different electrolyte concentrations. Figure 6.6.A shows V-I curves calculated based on the electrolyte concentrations shown in figure 6.5. It can be seen that for a lower concentration of electrolyte the cell shows a lower performance. Figure 6.6.B shows the power density for the same parameters.

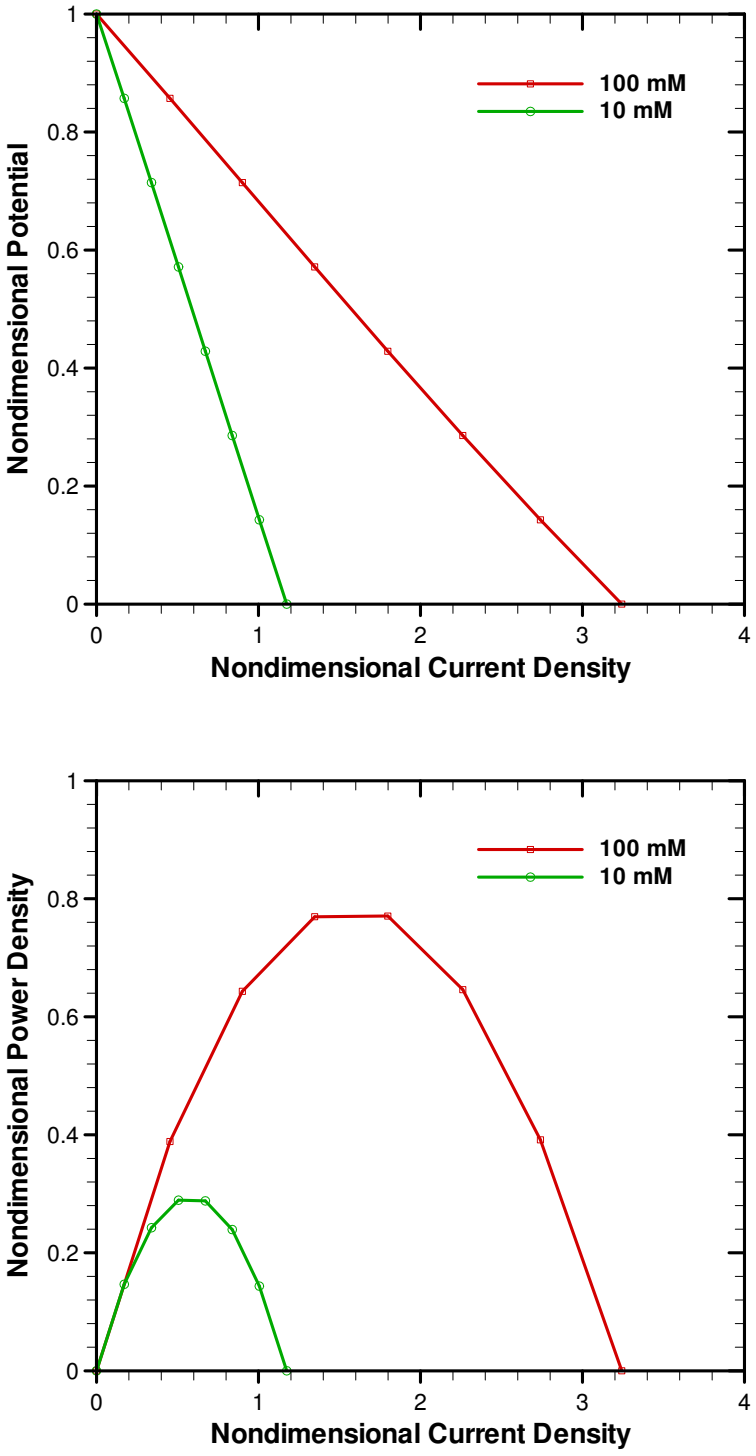

Figure 6.6 Performance Curves from LFFC Model at two different bulk electrolyte concentrations

Using the model to create the data in Figure 6.6 is essential to the usefulness of the simulation. It is this data that has to be compared to the experimental results. It can be seen that the model produces the same behavior as the experimental results presented earlier, meaning that it can be used to help predict and explain observed experimental results.

Another important performance consideration in fuel cells is the ohmic drop for the conduction of protons across the electrolyte. This fundamental model formulation for the electrostatic potential and ion species flux captures the necessary drop. Figure 6.7 shows an exaggerated y scale presentation of the potential distribution in the solution for two electrolyte concentrations at short circuit.

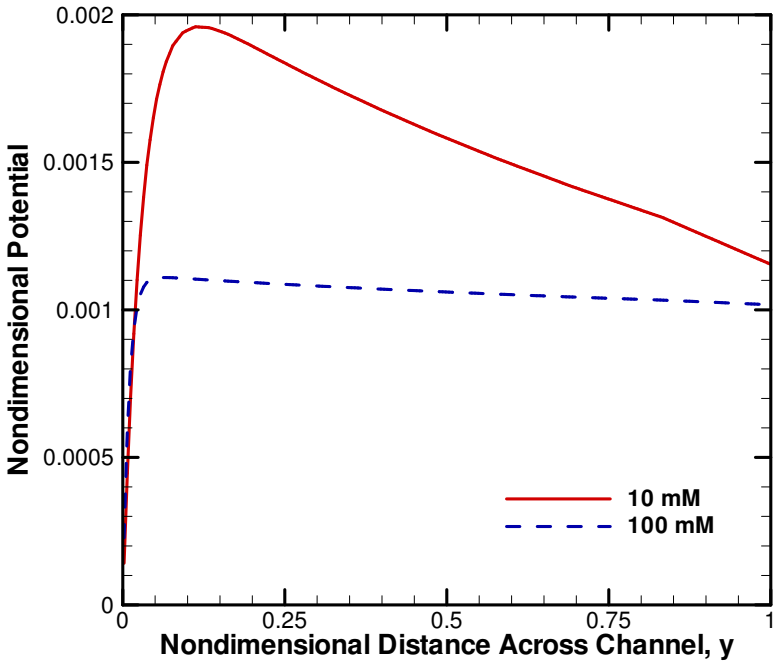

Figure 6.7 Exaggerated Y-Axis Scale to show the Ohmic Potential Drop due to proton conduction at short circuit for two different bulk electrolyte concentrations

It is noted that the profile is not flat like it would appear in Figure 6.3 but does in fact have the gradient necessary to move the protons in the solution. It breaks away from the linear ohms law at the interface where the double layer has to exist to balance out the charge. Also, the ohmic drop is greater for the electrolyte with lower concentration. This matches expected theory because a lower concentration of electrolyte has a greater resistance to ion conduction and therefore a larger potential drop.

CHAPTER 7

Conclusions

7.1 Fabrication and Proof of Device

A micro scale laminar flow fuel cell was fabricated on PDMS and its operating behavior characterized. Standard microfabrication techniques were used to create the device. It was operated as a direct methanol fuel cell, with oxygen saturated sulfuric acid as the oxidant. The fabricated cell was qualified as an operational device by running it as a full fuel cell. The performance was characterized by V-I curves and anode polarization plots. The LFFC produced net power at reasonable potentials for direct methanol fuel cell technology.

7.2 Stability Characterized

It was found that the device open circuit potential is not stable over extended operation. It was shown that the cell could be flushed, restarted and the same open circuit potential curve could be obtained. This concluded that the cause of this potential drop over long durations of time is therefore not caused by the permanent cell degradation with use. Instead it is related to a behavioral characteristic of LFFC operation. Future work would need to address the device instability phenomenon more specifically.

7.3 Flowing Electrolyte

To study the flow rate effect, 1M methanol solutions, either with the sulfuric acid or without it as the supporting electrolyte, were supplied to the anode. In particular, we

have investigated the effects of methanol flow rates in both the presence and absence of a strong electrolyte, H_2SO_4, on its anode performance in terms of anode current density, onset potential of methanol oxidation, solution resistance (R_{ele}), Anode charge transfer resistance, ($R_{andoe,ct}$) and anode double layer capacitance (C_{dl}). In the absence of H_2SO_4, we found that both the onset potential and $R_{andoe,ct}$ of methanol oxidation reaction increases as its flow rate increases. Changing values of the C_{dl} for different flow rate of the anode stream suggests that the anode double layer structure is significantly affected by the anode flow rate. We speculate that this change of the double layer structure and the resulting change in activation overpotential of electrokinetics over this double layer are the most likely causes of our observed decreasing methanol oxidation kinetics with an increasing flow rate of the anode stream in the absence of H_2SO_4. When 0.5M sulfuric acid is added to 1M methanol anode stream, we observe that the negative effects of high methanol flow rate on its oxidation kinetic is almost completely mitigated. We believe that the addition of 0.5M sulfuric acid dramatically decreases the width of the anode double layer. Its width is so thin in the presence of sulfuric acid that various flow rates of the anode stream do not significantly influence its width anymore, and hence that methanol oxidation kinetic does not decrease as the anode flow rate increases. Furthermore, with the addition of sulfuric acid to the anode stream containing 1M methanol, the methanol oxidation at the anode of our LFFC starts to show mass transport limited performance due to its increased oxidation kinetics.

7.4 Methanol Oxidation in a Laminar Flow Device

Methanol oxidation was shown to have a negative reaction order. The power output of the cell decreased as the concentration of methanol supplied to the anode was

increased. This was shown by the impedance spectroscopy to be a result of a negative concentration impact on methanol oxidation kinetics. It would appear that in the cell studied that increasing methanol concentration affects the structure of the electric double layer and therefore the kinetics. This effect is eliminated in the presence of a strong supporting electrolyte.

7.5 Analytical Model and Behavior of the EDL

Also, presented was behavior from analytical results that were very similar to observed behavior. To do this a model was developed that is more fundamental then the typical fuel cell model. By using the Poisson equation for electrostatic potential the proper potential and kinetic behavior can be described. The model was then used to simulate the basic performance trends of a laminar flow fuel cell. Although it does not explicitly show any trend based on flow rate it does show a good description of the basic fuel cell behavior. The role of the electric double layer in LFFC operation behavior can be clearly seen by the results. Also the mathematical model shows its power to analyze the core science behind the experimental results. Future work based on this thesis should follow this aspect of the work as it shows the most promise for revealing new information.

REFERENCES

[1] Jeffrey D. Morse 2007 Micro-fuel cell power sources *Int. J. Energy Res.* **31** 576–602

[2] R. Ferrigno, A.D. Stroock, T.D Clark, M. Mayer, and G.M. Whitesides 2002 Membraneless Vanadium Redox Fuel Cell Using Laminar Flow *J. Am. Chem. Soc.* **124** 12930-12931

[3] E.R. Choban, P. Waszczuk, L.J. Markoski, A. Wieckowski, and P.J.A. Kenis 2004 Microfluidic fuel cell based on laminar flow *Journal of Power Source* **128** 54-60

[4] E.R. Choban, P. Waszczuk, and P.J.A. Kenis 2005 Characterization of Limiting Factors in Laminar Flow-Based Membraneless Microfuel Cells *Electrochemical and Solid-State Letters* **8** (7) A348-A352

[5] J.L. Cohen, D.A. Westly, A. Pechenik, and H.D. Abruna 2005 Fabrication and preliminary testing of a planar membraneless microchannel *Journal of Power Source* **139** 96-105

[6] E. Kjeang, J. McKechnie, D. Sinton, N. Djilali 2007 Planar and three-dimensional microfluidic fuel cell architectures based on graphite rod electrodes *Journal of Power Sources* **168** 379–390

[7] E.Kjeang, R. Michel, D. A. Harrington, N. Djilali, and D.Sinton 2008 A Microfluidic Fuel Cell with Flow-Through Porous Electrodes *J. Am. Chem. Soc.* **130** 12 4000-4006

[8] S. Hasegawa, K. Shimotani, K. Kishi, and H. Watanabe 2005 Electricity Generation from Decomposition of Hydrogen Peroxide *Electrochemical and Solid-State Letters* **8** (2) A119-A121

[9] E. Kjeang, B. T. Proctor, A. G. Brolo, D. A. Harrington, N. Djilali, D. Sinton 2007 High-performance microfluidic vanadium redox fuel cell *Electrochimica Acta* **52** 4942–4946

[10] J.L. Cohen, D.J. Volpe, D.A. Westly, A. Pechenik, and H.D Abruna 2005 A Dual Electrolyte H_2/O_2 Planar Membraneless Microchannel Fuel Cell System with Open Circuit Potentials in Excess of 1.4 V *Langmuir* **21** 8 3544-3550

[11] E.R. Choban, J.S. Spendelow, L. Gancs, A. Wieckowski, and P.J.A. Kenis 2005 Membraneless laminar flow-based micro fuel cells operatin in alkaline acidic and acidic/alkaline media *Electrochimica Acta* **50** 5390-5398

[12] R.S Jayashree, L.Gancs, E.R Choban, A. Primak, D. Natarajan, L.J. Markoski, and P.J.A. Kenis 2005 Air-breathing Laminar Flow-Based Microfluidic Fuel Cell *J. Am. Chem. Soc. Vol.* **127** 48 16758-16759

[13] R.S. Jayashree, D. Egas, J.S. Spendelow, D. Natarajan, L.J markoski, and P.J.A. Kenis 2006 Air-Breathing Laminar Flow-Based Direct Methanol Fuel Cell with Alkaline Electrolyte *Electrochemical and Solid-State Letters* **9** (5) A252-A256

[14] E. Kjeang, A. G. Brolo, D. A. HarringtonN. Djilali and D. Sinton 2007 Hydrogen Peroxide as an Oxidant for Microfluidic Fuel Cells *Journal of The Electrochemical Society*, **154** 12 B1220-B1226

[15] K.G. Lim, G. Tayhas, and R. Palmore 2007 Microfluidic biofuel cells: The influence of electrode diffusion layer on performance *Biosensors and Bioelectronics* **22** 941-947

[16] M.H. Sun G. Velve Casquilas, S.S. Guo, J. Shi, H. Ji, Q. Ouyang, and Y. Chen 2007 Characterization of microfluidic fuel cell based on multiple laminar flow *Microelectronic Engineering* **84** 1182-1185

[17] A. Li, S. Hwa Chan and N. Nguyen 2007 A laser-micromachined polymeric membraneless fuel cell *Journal of Micromechanics and Microengineering* **17** 1107-1113

[18] J. Zhang, Y. Tang, C. Song 2006 PEM fuel cell open circuit voltage (OCV) in the temperature range of 23 ^{o}C to 120 ^{o}C *Journal of Power Sources* **163** 532-537.

[19] W. Jung, J. Han, S. Ha 2007 Analysis of palladium-based anode electrode using electrochemical impedance spectra in direct formic acid fuel cells *Journal of Power Sources* **173** 53-59.

[20] J. Qiao, M. Saito, K. Hayamizu 2006 Degradation of Perfluorinated Ionomer Membranes for PEM Fuel Cells during Processing with H2O2 *J. Electrochem. Soc.* **153** A967-A974.

[21] W. Chen, G. Sun, J. Guo, X. Zhao, S. Yan, J. Tian, S. Tang, Z. Zhou, Q. Xin 2006 Test on the degradation of direct methanol fuel cell *Electrochim. Acta* **51** 2391-2399.

[22] K. Furukawa, K. Okajima, M. Sudoh 2005 The behavior of palladium catalysts in direct formic acid fuel cells *Journal of Power Sources* **139** 9-14.

[23] T. Abe, H. Shima, K. Watanabe, Y. Ito 2004 Study of PEFCs by AC Impedance, Current Interrupt, and Dew Point Measurements. I. Effect of Humidity in Oxygen Gas *J. Electrochem. Soc.* **151** A101-A105.

[24] P. K. Das, X. Li, Z.-S. Liu 2007 Analytical approach to polymer electrolyte membrane fuel cell performance and optimization *Journal of Electroanalytical Chemistry* **604** 72–90

[25] S. Um, C.-Y. Wang, and K. S. Chenb 2000 Computational Fluid Dynamics Modeling of Proton Exchange Membrane Fuel Cells *Journal of The Electrochemical Society* **147** (12) 4485-4493

[26] W. Liu, C.-Y. Wang 2007 Electron transport in direct methanol fuel cells *Journal of Power Sources* **164** 561–566

[27] C.-Y.Wang 2004 Fundamental Models for Fuel Cell Engineering *Chem. Rev* **104** 4727-4766

[28] A. Z. Weber and J. Newman 2004 Modeling Transport in Polymer-Electrolyte Fuel Cells *Chem. Rev.* **104** 4679-4726

[29] J. Wu, V. Srinivasan, J. Xu and C. Y. Wang 2002 Newton-Krylov-Multigrid Algorithms for Battery Simulation *Journal of The Electrochemical Society* **149** A1342-A1348

[30] B. L. García, V. A. Sethuraman, J. W. Weidner, R. E. White 2004 Mathematical Model of a Direct Methanol Fuel Cell *Journal of Fuel Cell Science and Technology* **1** 43-48

[31] Z. H. Wang and C. Y. Wang 2003 Mathematical Modeling of Liquid-Feed Direct Methanol Fuel Cells *Journal of The Electrochemical Society*, **150** A508-A519

[32] S. F. Baxter, V. S. Battagli and R. E. White 1999 Methanol Fuel Cell Model: Anode *Journal of The Electrochemical Society,* **146** (2) 437-447

[33] M.R. Shivhare, C.L. Jackson, K. Scott , E.B. Martin 2007 Simplified model for the direct methanol fuel cell anode *Journal of Power Sources* **173** 240–248

[34] M.R. Shivhare, R.G. Allen, K. Scott , A.J. Morris, E.B. Martin 2006 A kinetic model for the direct methanol fuel cell anode based on surface coverage *Journal of Electroanalytical Chemistry* **595** 145–151

[35] K. Scott, P. Argyropoulos 2004 A one dimensional model of a methanol fuel cell anode *Journal of Power Sources* **137** 228–238

[36] A. Bazylak, D. Sinton, and N. Djilali 2005 Improved fuel utilization in microfluidic fuel cells: A computational study *Journal of Power Source* **143** 57-66

[37] M. Chang, F. Chen, N. Fang 2006 Analysis of membraneless fuel cell using laminar flow in a Y-shaped microchannel *Journal of Power Sources* **159** 810-816

[38] F. Chen, M.H. Chang, and M.K. Lin 2007 Analysis of membraneless formic acid microfuel cell using a planar microchannel *Electrochimica Acta* **52** 2506-2514

[39] Z. Zheng D. J. Hansford A. T. Conlisk 2003 Effect of multivalent ions on electroosmotic flow in micro- and nanochannels *Electrophoresis* **24** 3006–3017

[40] M. Z. Bazant, K. Thornton and A. Ajdari 2004 Diffuse-charge dynamics in electrochemical systems *Physical Review* E **70** 021506

[41] W. D. Murphy J. A. Manzanares S.Mafe and H. Reiss 1992 A Numerical Study of the Equilibrium and Nonequillbrlum Diffuse Double Layer in Electrochemical Cells *J. Phys. Chem.* **96** 9983-9991

[42] M. Z. Bazant, K. T. Chu, and B. J. Bayly 2005 Current-Voltage Relations for Electrochemical Thin Films *SIAM J. APPL. MATH* **65** (5) 1463–1484

[43] A. Bonnefont, F. Argoul, M. Z. Bazant 2001 Analysis of diffuse-layer effects on time-dependent interfacial kinetics *Journal of Electroanalytical Chemistry* **500** 52-61

[44] James J. Allen 2005 *Micro Electro Mechanical System Design* (Boca Raton, Taylor & Francis Group) p115-148

[45] E. Barsoukov, J. R. Macdonald, 2005 *Impedance Spectroscopy Theory, Experiment, and Applications Second Edition* (Hoboken NJ, Wiley Inter-Science)

[46] R. F. Ismagilov, A.D Stroock, P.J.A. Kenis, and G. Whitesides 2000 Exeperimental and theoretical scaling laws for transverse diffusive broadening in two-phase laminar flows in microchannels *Appl. Phys. Lett.* **76** 17, 2376-2378

[47] A.V. Tripkovic, K.D. Popovic, B.N. Grgur, B. Blizanac, P.N. Ross, and N.M. Markovic 2002 Methanol electrooxidation on supported Pt and PtRu catalysts in acid and alkaline solutions *Electrochimica Acta* **47** 3707-3714

[48] J. Newman, K. E. Thomas-Alyea 2004 *Electrochemical Systems Third Edition* (Hoboken NJ, Wiley Inter-Science)

[49] J. Bockris, A. K. N. Reddy 1970 *Modern Electrochemistry; an Introduction to an Iinterdisciplinary Area* (New York, Plenum Press)

[50] H. Wang, H. Baltruschat 2007 DEMS Study on Methanol Oxidation at Poly-and Monocrystalline Platinum Electrodes: The Effect of Anion, Temperature, Surface Structure, Ru Adatom, and Potential *J. Phys. Chem.* **111** 7038-7048.

[51] S. Patankar 1980 *Numerical Heat Transfer and Fluid Flow* (Taylor&Francis)